

# Gas Tube Design, by H H Wittenberg

From: **Electron Tube Design**, RCA Electron Tube Division, 1962, pages 792 - 817.

## Gas Tube Design

H. H. Wittenberg

Lancaster

The subject of gas tubes is an old one. Early electron tubes were gassy due to inadequate pumping techniques. Certain early amplifier tubes, on the other hand, were gas-filled in an attempt to use the gain resulting from avalanche ionization; early cathode-ray tubes also were gas-filled to assist focusing. The gas tube field enjoyed a heyday in the late 1920's when the phanotron (low-pressure gas diode), tungar (high-pressure gas diode), thyatron, and ignitron appeared in quick succession. The gas-tube field was quiescent during the thirties while vacuum tube development surged ahead. During World War II the transmit-receive (TR) box and the hydrogen thyatron made radar practical and revived interest in the gas-tube field. In the early 1950's, the gas-tube field received another "shot in the arm" with the developments of the Plasmatron and Tacitron by our Princeton Laboratories. At this writing the fusion process for releasing nuclear energy again focuses attention on gas tubes.

The theory upon which the foregoing devices are based exhibits a similar chronology. Townsend originated the early theory in 1915. Langmuir, Hull, and Slepian developed, in about 1929, the basic theory which is currently found in the text books. Because much of the phenomena are not yet understood, contemporary researchers, including S. C. Brown, S. T. Martin, L. Malter, and E. O. Johnson, using modern techniques, are now developing new and more comprehensive theory.

The gas tube is often thought of as being limited to the audio range in its frequency of operation; on the contrary, some gas tube phenomena occur at megacycle rates. TR boxes involve the radar frequencies, measurement techniques utilize ultrahigh frequency (UHF), and the yet unharnessed oscillations inherent in a gas discharge extend into the VHF spectrum.

The complexity of the gas tube may be ascribed to the fact that three types of particles are involved: molecules, ions, and electrons. Further complications arise from the varieties and combinations of gases which may make up the molecules and ions.

Although the gas-tube designer is spared the necessity of mastering certain vacuum-tube operational characteristics, he must be familiar with many techniques and characteristics of the vacuum-tube field such as pumps and exhaust, gettering, heaters, emission and coatings, anode materials, heat radiation and conduc-

tion, grid emission, and amplification factor. In addition, he must master the techniques of gas filling and understand the complex phenomena resulting therefrom. The scope of the material in this article is restricted to phenomena unique to gas tubes.

### PROCESSES PRIOR TO CONDUCTION

#### Collision

**Mean-Free-Path.** Gas molecules may be ionized by electron impact. This process is of major importance since, when coupled with secondary emission of electrons from the cathode, it makes possible a self-sustaining gas discharge. An electron injected into a gas will collide with the gas molecules. If the molecules were spaced in an orderly array, such that along a given straight line the spaces between molecules were equal and the electron continued along this same straight line between collisions, then the free path between collisions would be a constant length. But the molecules are in motion and the electron direction is random and subject to change after every collision. Consequently, the free path of a given electron is continually changing.

The mean of this variable-length path can be found in the following manner (see Fig. 1). In traveling a free path through the gas, the electron may be imagined to cut a cylindrical path of cross-sectional area  $\pi r^2$ , where  $r$  is the molecular radius. If the center of the molecule lies within this path, it will be hit when the electron has traveled a length  $\lambda$ , called the mean free path.

When the unit volume of the path of the electron is equated to the unit volume per molecule:

$$\lambda \pi r^2 = 1/N \quad (1)$$

where  $N$  is the number of molecules per unit volume.

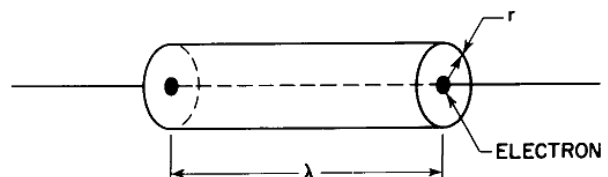


Figure 1. Mean Free Path of Electrons

The molecular mean free path, derived in a similar manner, is found to be 1/4 of the electron mean free path.<sup>1</sup> Because molecular speed is much lower than electron speed, the second or target molecule will have moved during the free flight of the first molecule. A more rigorous calculation taking this thermal motion into account gives the molecular free path,

$$\lambda_m = 1/4\sqrt{2} \lambda_e \quad (1a)$$

where  $\lambda_e$  is the electron mean free path.

The molecule collides more frequently per given distance of travel.

By the gas laws:

$$N = PV/kT \quad (2)$$

where P = pressure (dynes/cm<sup>2</sup>)  
 V = volume (cm<sup>3</sup>)  
 T = temperature, degrees Kelvin  
 k = Boltzmann's Constant (1.38 x 10<sup>-16</sup> erg/deg)

Hence, the mean free path is proportional to the absolute temperature of the molecules and inversely proportional to the pressure of the molecules. Table I gives the mean free path of the gases used in gas tubes at a typical dosing pressure.<sup>2</sup>

TABLE I. Mean Free Path

Gas	Mean Free Path in millimeters*	
	For Molecule	For Electron In Gas
H <sub>2</sub>	0.90	5.1
He	1.41	8.0
Ne	1.00	5.66
A	0.51	2.88
Kr	0.39	2.2
Xe	0.26	1.47
Hg	0.35 (100 μ, 82 C)	1.98
	3.5 (10 μ, 47 C)	19.8
	35.0 (1 μ, 18 C)	198.0

\*Note: At 0 C and 100 microns (μ) pressure except as indicated

Free Paths vs. Number of Particles.<sup>3</sup> Because the motion of gas molecules is random, the free paths are randomly distributed with regard to distance. Some paths are long while others are short. Since  $\lambda$  is the mean free path of the electron,  $1/\lambda$  is the mean collision frequency (collisions per centimeter) per electron. The number of electrons  $dn$  colliding while traversing

a distance  $dx$  is:

$$dn = -n \frac{1}{\lambda} dx \quad (3)$$

where  $n$  = number of electrons traveling distance  $x$  without collision

The negative sign signifies the decrease in  $n$  as  $x$  is increased.

Integrating Eq. (3) and substituting boundary conditions gives:

$$n = n_0 e^{-x/\lambda} \quad (4)$$

where  $n_0$  = total number of electrons

This is known as the survival function and describes the number of electrons surviving in their original path without collision after traveling distance  $x$ . It is more valuable to know the number of electrons having free paths in the range of  $x$  to  $(x + dx)$ . Differentiating Eq. (4) with respect to  $x$  gives:

$$\frac{dn}{dx} = -\frac{n_0}{\lambda} e^{-x/\lambda} \quad (5)$$

To use this relationship, the differentials are replaced by increments and regrouped to give

$$\frac{\Delta n}{n_0} = -\frac{x}{\lambda} e^{-x/\lambda} \quad (6)$$

Eq. (6) is plotted in Fig. 2. Note that in this case the distribution function of Eq. (6) is the same as the survival function of Eq. (4).

To better appreciate these relationships, the distribution function of men's heights may be plotted, as in Fig. 3, corresponding to the function of Eq. (4), but having a different shape. If knowledge of the number of men

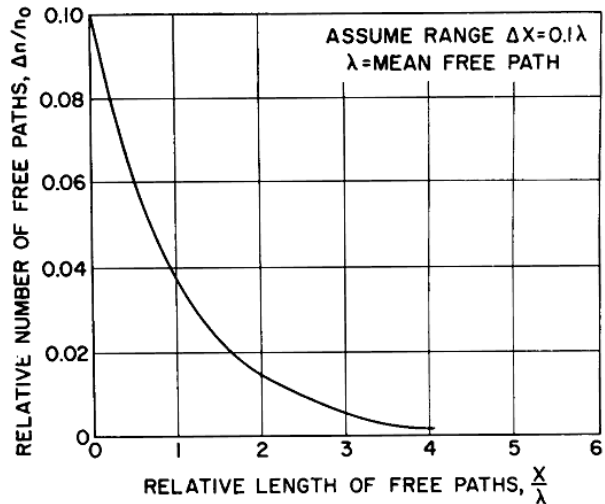


Figure 2. Distribution of Free Paths

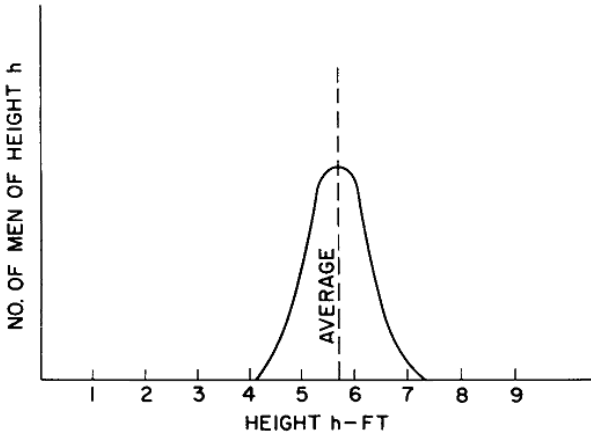


Figure 3. Distribution of Men's Heights

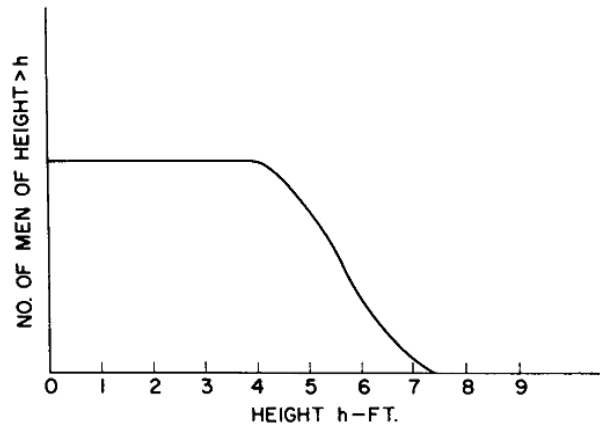


Figure 4. Integrated Distribution of Men's Heights

with heights greater than a given value  $h$  is desired, Fig. 3 may be integrated to get Fig. 4. Fig. 4 is the survival curve corresponding to the function of Eq. (4).

Examination of Fig. 2 shows that 10 per cent of the free paths are in the range of 0 to 0.1 of the mean free path  $\lambda$ . Very few electrons have paths greater than  $\lambda$ ; only 3.7 per cent have free paths in the range centering at  $\lambda$ .

**Free Paths vs. Voltage.** If the electrons and molecules are considered as solid spheres, it would appear that the mean free path were independent of speed of the moving particles. However, if the molecule is pictured as a planetary system of electrons, it is easy to imagine that a fast moving electron may miss the planetary electrons and so avoid collision. Experimental evidence shows that the mean free path is, indeed, a function of speed  $S$ . It is customary to express this function<sup>4</sup> in terms of the mean collisions per unit distance  $P_C$  and voltage  $V$  (see Fig. 5). The reciprocal of  $P_C$  is the mean free path. This quantity  $P_C$  has been miscalled probability of collision, but is not a probability since it has dimension 1/centimeter. From Eq. (1) it can be seen that  $1/\lambda$  is proportional to the cross section and hence is sometimes expressed as collision cross section.

Voltage is related to speed by the formula

$$S = \left( \frac{2qV}{m} \right)^{1/2} \text{ meters/sec} \quad (7)$$

where  $q$  = charge of particle in coulombs  
 $m$  = mass of particle in kilograms

The arrows in Fig. 5 show the kinetic-theory values which were calculated using only the speed of thermal motions (equivalent to fractions of a volt).

Ionization

**Voltage Dependence.** Having collided with an atom, the colliding electron may affect the planetary electrons

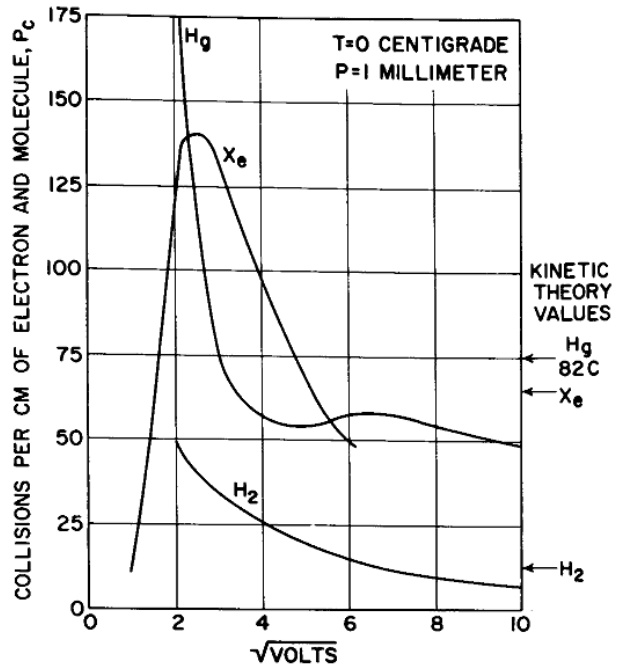


Figure 5. Probability of Collision

in the following ways:

- (a) A planetary electron may be excited, remain so for about  $10^{-9}$  second, and then radiate the energy received in the collision.
- (b) A planetary electron may be excited, remain so for  $10^{-3}$  second (metastable), and suffer a second collision from which it may be removed from the atom (cumulative ionization).
- (c) A planetary electron may be removed directly (ionization).

(d) The electron may simply bounce off like a pea from a cannon ball.

Table II gives critical voltages at which effects described in (a) through (c) begin to occur.

**Probability of Ionization.** Like the probability of collision, the probability of ionization actually is not a probability but a coefficient. It is expressed as ions per centimeter per colliding particle. (Townsend labeled this coefficient  $\alpha$ .) The ionizing coefficient is shown in Fig. 6 as a function of voltage.<sup>5</sup> Above the threshold values (shown in Table II), the probability of ionization increases to a peak and then falls. It will be noted that the ionization coefficient is maximum at about five times the threshold ionization voltage.

## BREAKDOWN

### Secondary Emission at Cathode

Assume that two parallel plane electrodes, immersed in a gas, have a voltage applied to them. Stray radiation striking the negative electrode will release a small number of electrons. The electrons move toward the positive electrode and further ionize in a manner just described. Likewise, the ions move toward the negative electrode colliding frequently with molecules, but few ions are produced in such collisions.<sup>6</sup> However, upon hitting the negative electrode the ions are effective in releasing electrons by the process of secondary emission (Townsend labeled this coefficient of this process  $\gamma$ ). Fig. 7 is a graph<sup>7</sup> of the secondary emission vs. the electric field (in volts per centimeter) for hydrogen

TABLE II. Critical Voltages of the Gases<sup>17, 18</sup>

Gas	Weight	Vapor Pressure*	First Ionization Voltage Volts	Second Ionization Voltage Volts	Excitation Voltage Volts	Metastable Voltage Volts
Cs	55	$5 \times 10^{-4}$	3.9	23.4	1.4	
Rb	37	$1 \times 10^{-4}$	4.2	27.4	1.5	
K	19	$2 \times 10^{-5}$	4.3	31.7	1.6	
Na	11	$1 \times 10^{-7}$	5.1	47.1	2.1	
Li	3	$10^{-8}$	5.4	75.3	1.8	
Ca	20	$10^{-8}$	6.1	11.8	2.5	1.9
Mg	12	$10^{-8}$	7.6	15.0	4.3	2.7
Hg	80	$3 \times 10^{-1}$	10.4	18.1	4.9	4.7, 5.4
Xe	54		12.1	21.1		8.3, 8.9
H <sub>2</sub> O	18		13.2		17.6	
H	1		13.4		10.1	
Kr	36		13.9	26.4		9.9, 10.5
O <sub>2</sub>	32		14.1		6.1	
CO	28		14.2		6.0	3.5
CO <sub>2</sub>	44		14.3		10.0	
H <sub>2</sub>	2		15.3		11.1	
A	18		15.7	27.8		11.5, 11.7
N <sub>2</sub>	28		16.7		8.5	
Ne	10		21.5	40.9		16.6, 16.8
He	2		24.5	54.1		19.7, 20.5

\*Note: Vapor pressure in mm Hg at 100 C

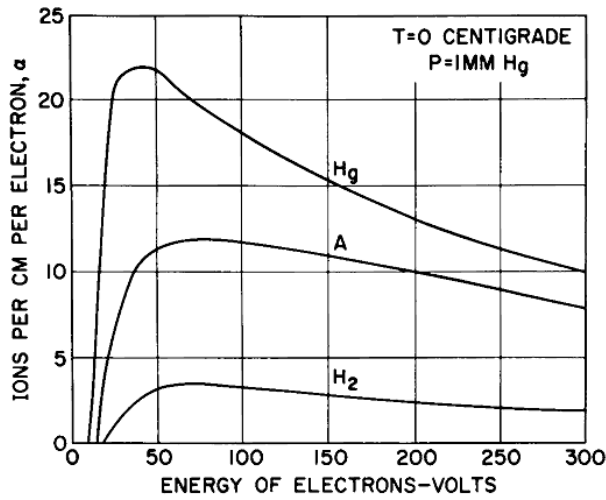


Figure 6. Probability of Ionization

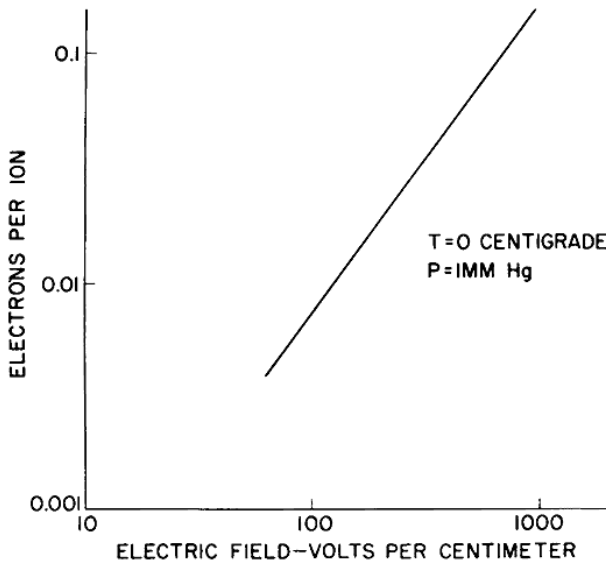


Figure 7. Secondary Ion Emission

with zinc electrodes. If the two processes of ion production by electron collision with a molecule and electron production by ion impact at the cathode are combined, the elements of a feedback system are perceived to be present. If the gain of the system exceeds one, the result is breakdown of the gas. Limitations in the form of external resistance and ion losses with the gas-filled envelope prevent unlimited current build-up and stabilize the gas discharge in various modes to be described later. See Appendix A for a mathematical treatment of current build-up.

Paschen's Law

The voltage at which the ion-electron generation sys-

tem feedback becomes unstable is called the breakdown voltage. It is common experience that at atmospheric pressure the breakdown voltage decreases as the distance between electrodes is decreased. It is not common knowledge that at low gas pressures the distance can be decreased to a point where the breakdown voltage reaches a minimum and thereafter increases as the distance is further decreased. The complete relationship between breakdown voltage, distance, and pressure was first discovered by F. Paschen in 1889 and is known as Paschen's Law.

Paschen's Law may be deduced in a nonmathematical fashion. Referring to Fig. 8, the line labeled "Collisions per Electron in Traversing  $X_a$ " rises with increasing pressure because the gas density increases with pressure and consequently there are more molecules inserted in the path of the traveling electron. The line labeled "Energy per Collision" falls as pressure increases, because (assuming that the electron loses all of its energy at each collision) the electron has a shorter distance between collisions to pick up energy from the electric field. As was shown previously, because a certain energy must be acquired to produce ionization on impact, the total number of ions produced must be a product of these two values. This product is shown as the curve "Ions Produced". It has a maximum near the crossover of the two lines. The more ions that are produced, the less voltage is necessary to cause breakdown. Hence, the breakdown voltage curve has a minimum. A similar reasoning process can be carried through for distance as a variable, with pressure constant. In the complete Paschen's Law, breakdown voltage is a function of the product of distance and pressure (pd). A plot of Paschen's Law exhibits the same shape as the curve in Fig. 8. Plots of Paschen's Law for the various gases, have different minimums as Fig. 9 shows, but all exhibit the same characteristic shape. A mathematical derivation of Paschen's Law is given in Appendix B.

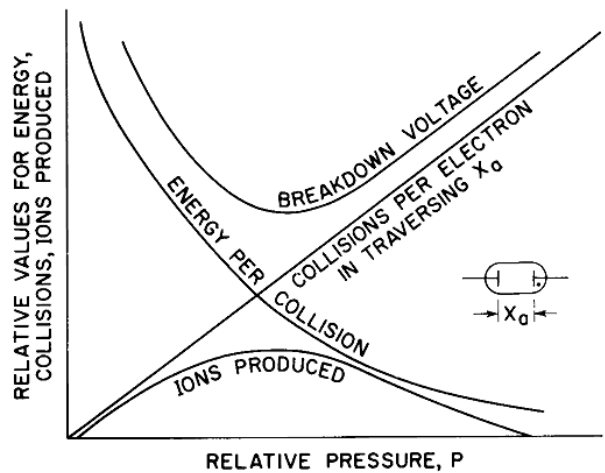


Figure 8. Non-mathematical Derivation of Paschen's Law

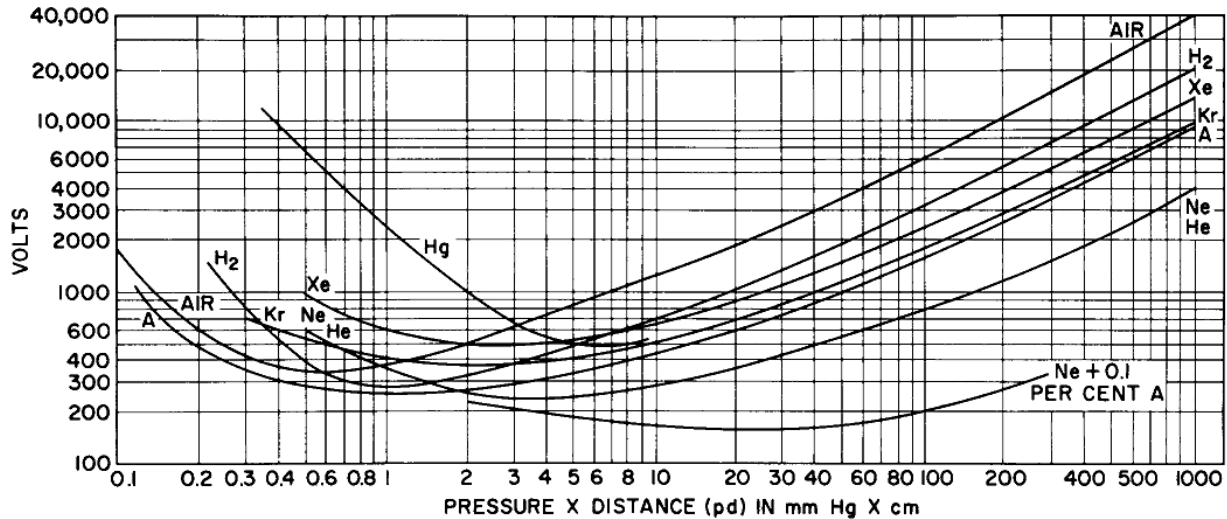


Figure 9. Paschen's Law for Various Gases

PROCESSES DURING CONDUCTION

Voltage vs. Current

Fig. 10 shows the voltage-vs.-current relationship for a gas discharge. As the voltage is increased from zero, a small current called the Townsend current flows. Ionization gauges operate in this region and the gas test for vacuum tubes is performed here. With irradiation of the cathode, the curve shifts to higher currents as shown by the dotted curve. Gas phototubes are operated in this region and realize the benefits of gas amplification. Geiger-Mueller (GM) tubes also operate in this region and indicate the presence of cathode irradiation by current increases. At further increases in supply voltage, a plateau is encountered; such a flat characteristic permits the use of a gas-filled tube as a corona-type gas voltage regulator. Although in Fig. 10 the plateau is at about 400 volts, different gases and different electrode materials can shift this region upward to several kilovolts.

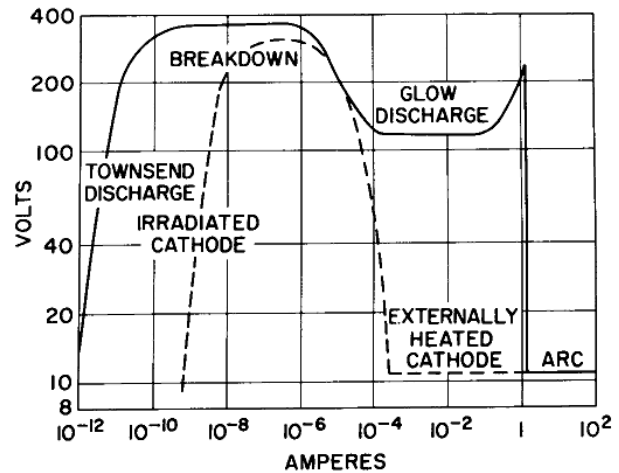


Figure 10. Voltage vs. Current

On the plateau just described breakdown occurs which, without the limitation of a series resistance, will result in an uncontrolled increase of current. Large series resistance and a large supply voltage permit the negative resistance portion to be traversed. Farther along the solid line is the glow-discharge region. In this region the glow-discharge voltage regulators (VR tubes) and the transmit-receive switches (TR tubes) are operated. Cathodes of such tubes are relatively cold and emission occurs by virtue of ion bombardment.

Voltage vs. Distance

Further increases of current lead to the sudden drop of terminal voltage to about 10 volts. A very low voltage and an incandescent cathode are characteristic features of the arc discharge. If the cathode is externally heated, the glow discharge mode is bypassed and the low voltage region is entered immediately. It is in this region that the thyratrons and hot-cathode gas rectifiers operate.

In a vacuum diode having parallel plane electrodes, the voltage<sup>8</sup> is proportional to the 4/3 power of the distance between cathode and anode; the slight deviation from linearity is a result of the negative electron space charge. In a gas diode having parallel plane electrodes, the voltage distribution with distance may take several modes depending upon (1) whether the negative-electron or the positive-ion space charge predominates and (2) upon boundary conditions. Fig. 11 shows three of the voltage distributions<sup>9</sup> which have been identified. The Langmuir mode is characterized by a sharp rise within about a millimeter of the cathode and a practically constant voltage from there to the anode. Visually, the region next to the cathode (identified as the "sheath") is dark, indicating the absence of excited atoms and ions. The remainder of the volume (identified as the

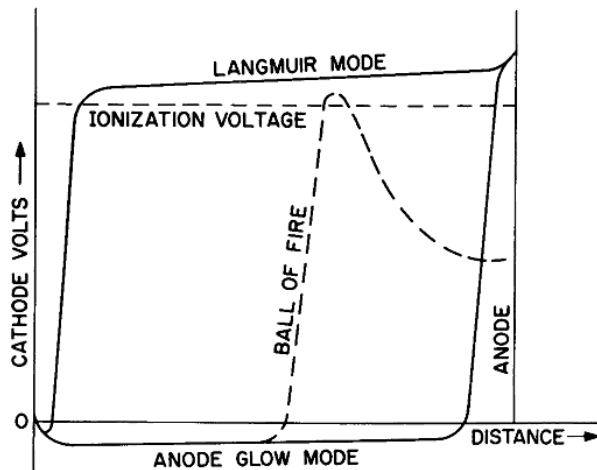


Figure 11. Voltage vs. Distance

"plasma") glows indicating the presence of excited atoms and ions. The sheath draws electrons from the cathode and accelerates them to sufficient velocity for ionization. The existence of this sheath makes possible the design of gas-tube cathodes with several times the thermal efficiency of vacuum-tube cathodes.

The Langmuir mode is most common in typical gas tubes. When the anode current in a typical gas tube is reduced to a small percentage of the available emission (as determined in a vacuum) the anode-glow mode<sup>10</sup> may be observed. As Fig. 11 shows, the sheath occurs close to the anode. The electrons enter the field-free region from the cathode as a result of initial velocities. The anode-glow mode may be enhanced by increasing pressure above 300 microns and by minimizing ion losses. The inverted structure in which the cathode surrounds the anode is capable of operating in the anode-glow mode to higher anode currents than conventional structures. The Tacitron, designed to operate in this mode, exhibits advantages of low noise and current cutoff ability.

At current levels intermediate between the Langmuir mode and the anode-glow mode, the ball-of-fire mode is encountered. As may be seen in Fig. 11, the voltage rises to a maximum as the point of observation progresses across the tube. With such a distribution the maximum voltage may be sufficient to ionize whereas the over-all voltage across the tube may be appreciably less.

#### Sheath

A sheath in a gas tube is defined as a region exhibiting appreciable electric field. Its thickness is small compared to the mean free path so that electrons and ions cross the sheath without collision. In the sheath just described, electrons emitted from the cathode enter the sheath on one side, whereas ions emitted from the plasma enter the sheath on the other side. Such a sheath is actually called a double sheath. The single sheath, which involves charges of only one kind,

is the simplest mathematically and so will be considered first. The mathematical solution to the single sheath case is identical to the solution of the space-charge-limited vacuum-diode case, known as Child's Law.<sup>11</sup>

$$i = 5.23 \cdot 10^{-8} M^{-1/2} d^{-2} V^{3/2} \quad (9)$$

where  $i$  = current in amperes per square centimeter  
 $M$  = atomic weight of ion  
 $d$  = thickness of sheath in centimeters  
 $V$  = voltage across sheath in volts

This formula holds for the case of an electrode immersed in a plasma. Application of a voltage to such an electrode causes the sheath to be formed. The plasma serves as the emitter of positive ions which move across the sheath to the electrode. The density of the current to the electrode is identical to the density of the current across a surface in the plasma (assuming the electrode to be large with respect to the sheath thickness). It will be seen later that the plasma current density is fixed by the conditions of the plasma and, to also satisfy Child's Law, the thickness of the sheath adjusts itself. A double sheath exists when electrons enter the source from one side and ions enter the sheath from a source on the other side. Consider the sheath to occupy the entire space between cathode and anode, which means that electrons cross the sheath and collide with gas molecules directly in front of the anode. A mathematical solution to this double sheath problem<sup>12</sup> shows that the current in the external circuit is 86 per cent greater for the gas-filled device than for the vacuum device. This increased current consists of 98 per cent electrons and 2 per cent ions. The ions contribute little because they move slowly, but they reduce the negative space charge permitting the larger electron flow.

If the circuit voltage is increased, the current increases and the sheath thickness decreases to less than the anode-to-cathode distance. A plasma develops in the vacated space between the sheath and the anode. Because the plasma is a region of high conductivity, this case may be described as one in which a virtual anode exists at the sheath boundary. In comparison, the current flow for the vacuum diode would increase with a decrease of anode-to-cathode distance. Mathematical considerations show that the current for the gas-filled device is always 86 per cent greater than that for the vacuum diode if the anode in the vacuum diode is placed at the same distance from the cathode as the virtual anode is in the gas diode. In actual tubes, this procedure is impractical because the sheath generally reduces across to a millimeter or less.

#### Plasma

Description. The plasma may be defined as a region of very small electric field. The electron and positive ion densities are approximately equal. For example, in mercury at a pressure of 1 micron, a discharge of 170 milliamperes per square centimeter has  $10^{11}$  ions per cubic centimeter,  $10^{11}$  electrons per cubic centimeter, and  $4 \times 10^{13}$  atoms per cubic centimeter. Note that only one out of 4000 atoms is ionized. The atoms move about as a result of their thermal energy which is relatively low<sup>13</sup> (0.04 volts at 25 C).

Recombination of an electron and an ion in the plasma is rare because the electron is unable to dispose of its kinetic energy in the collision with the heavier ion. See Appendix C for the mathematics of this process.

Ions and electrons can combine easily at the walls of a discharge tube. When a particle of either kind strikes a wall, it gives up its kinetic energy as heat and adheres by electrostatic attraction until a particle of the opposite sign arrives to form a neutral atom.

**Velocity Distribution.** To analyze the behavior of the plasma it is necessary to determine the velocity distribution of the particles therein. In the literature<sup>14</sup> may be found the theory which culminates in the following function:

$$f(V_x^2) = A_1 e^{-A_2 V_x^2} \tag{10}$$

where  $V_x$  = component of velocity in x-direction  
 $f(V_x^2)$  = fraction of particles having speeds in range  $dV_x$  divided by  $dV_x$

$$A_1 = \left(\frac{m}{2\pi KT}\right)^{1/2}$$

$$A_2 = \frac{m}{2KT}$$

$m$  = mass of particle  
 $K$  =  $1.38 \times 10^{-23}$  joule per degree  
 $T$  = temperature in degrees Kelvin

This function is plotted in Fig. 12 for hydrogen. The curves show that the most probable velocity component in the x-direction is zero, but the resultant velocity is not zero because the velocities  $V_y$  and  $V_z$  in the other directions probably are not zero. Note that the distribution is a function of  $V_x^2$  and is, therefore, the same in both the positive and negative directions. As the temperature is increased, the number of particles having higher velocities increases, but the area under the

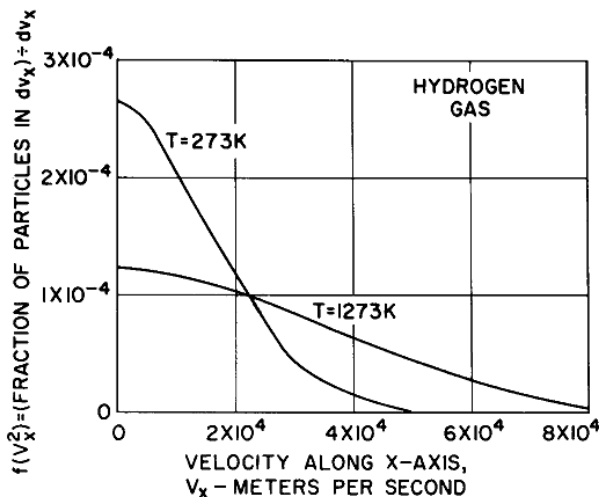


Figure 12. Velocity Distribution (Hydrogen gas)

curve (the total number of particles in the given volume) remains constant.

The temperature of the ions is about the same as that of the molecules of the gas (a few hundred degrees Kelvin); both types of particles collide among themselves and with each other, and thereby interchange energy. The electrons are found to have a much higher temperature than the ions or molecules (in the tens of thousands of degrees Kelvin).

**Particles Crossing Plane.**<sup>15</sup> To determine the number of particles crossing a sheath, it is necessary to know how many particles cross a unit area (ABCD of Fig. 13) in one direction. All of the particles in the box of height  $V_x$  and base ABCD, having velocities in the range  $V_x$  to  $(V_x + dV_x)$ , will cross area ABCD in one second. Of course, some of the particles starting at the far end of the box will leave the box because of  $y$  and  $z$  components of velocity, but they will be replaced by an equal number of outside particles. The total number of particles in the box is given by

$$n_v = N \cdot V_x \cdot l \tag{11}$$

where  $N$  = density of particles

Utilizing the velocity distribution function of Eq. (10) to obtain the number of particles in the box having velocities between  $V_x$  and  $(V_x + dV_x)$  gives

$$dn_v = NV_x A_1 e^{-A_2 V_x^2} \tag{12}$$

where the constants  $A_1$  and  $A_2$  are functions of the temperature and of the gas only

To find the total number of particles crossing the unit area per second, it is necessary to integrate over all velocities (0 to  $\infty$ ) giving

$$n_{0,\infty} = NA_1 \int_0^\infty V_x e^{-A_2 V_x^2} dV_x \tag{13}$$

or

$$n_{0,\infty} = \frac{NA_1}{2A_2} = \left(\frac{KT}{2m\pi}\right)^{1/2} \tag{14}$$

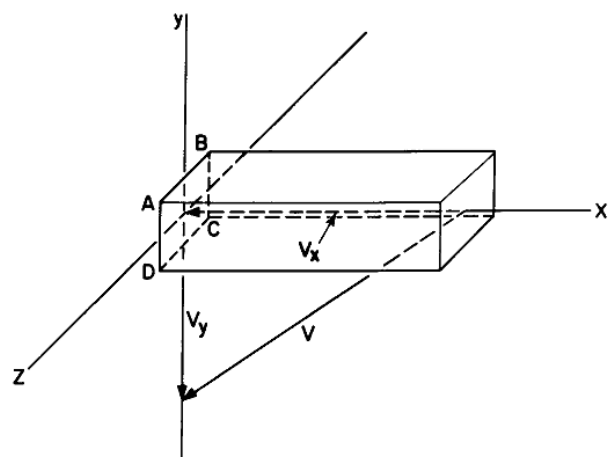


Figure 13. Particles Striking Wall

Multiplying the number of particles crossing the unit area per second by the charge per particle gives the random plasma current density  $J_r$ . Useful in the analysis of sheaths is the expression for the number of charged particles crossing the unit area against a retarding voltage. The particle must have a kinetic energy ( $1/2mV_x^2$ ) equal to or greater than the potential energy  $qE$  (where  $q$  is the charge and  $E$  the voltage):

$$1/2mV_x^2 = qE \tag{15}$$

Substituting  $V_x$  for the lower limit instead of zero and integrating gives

$$n_{v,\infty} = n_{0,\infty} e^{\frac{-mV_x^2}{2KT}} \tag{16}$$

$$= n_{0,\infty} e^{\frac{-qE}{KT}} \tag{17}$$

**Probes.** The insertion of a third electrode in a gas discharge between cathode and anode sets the scene for a situation known as "probe behavior." If the voltage of the third electrode or probe is varied with respect to the cathode, the current will vary in the manner shown in Fig. 14. When the voltage of the probe is more than a few volts below that of the cathode (line A-B), the current is small and at saturation level; the direction of the current and the saturation shows that the probe is collecting positive ions only. Similarly, along line C-D, the probe is collecting only electrons. These saturation effects are accompanied by sheaths which surround the probe and expand (see Eq. (9) and discussion on sheaths) as the voltage between the probe and the plasma increase.

Along line B-C, the probe is collecting both positive ions and electrons. When the probe current is zero, the numbers of ions and electrons collected are equal. The corresponding voltage  $F$  is not the space voltage, but is some negative value since the faster moving electrons must be repelled to equalize the numbers of both particles collected.

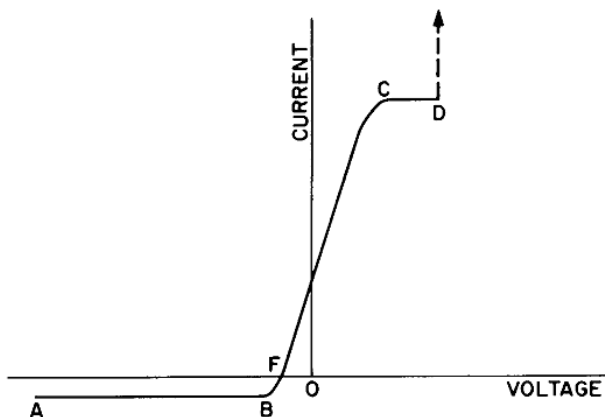


Figure 14. Probe Characteristic

As long as the probe voltage is less than the space voltage, the positive-ion current remains constant. Starting at B and making the voltage more positive, the electron current  $I_e$  increases according to the following modification of Eq. (17)

$$I_e = n_{0,\infty} S q e^{\frac{-qE}{KT_e}} \tag{18}$$

where  $S$  = area of probe

$q$  = charge

$T_e$  = electron temperature

$E$  = voltage difference between probe and space

Taking the logarithms of Eq. (18)

$$\ln I_e = \ln A_3 - \frac{q}{KT_e} E \tag{19}$$

When the experimental data are substituted in Eq. (19) and plotted, the straight-line portion gives the electron temperature  $T_e$ . The voltage at which the plot departs from a straight line is considered to be space voltage. At a more positive voltage, the positive-ion space charge disappears and a negative electron space charge appears. With  $T_e$  determined and assuming saturated electron current, Eq. (14) can be used to obtain the electron density  $N_e$ . The positive ion density is  $N_p = N_e$ .

Although a value for ion temperature can be determined by applying Eq. (14) to ions, the value thus determined is higher than the gas temperature, which is considered to be the correct value for ion temperature.

RECTIFIERS

Anode Efficiency

The efficiency of the hot-cathode gas rectifier accounts for its nearly exclusive use in the application range of 1000 to 20,000 peak inverse volts. For average currents from 0.1 ampere to 10 amperes, the gas tube displays a low tube drop (about 10 volts), whereas the drop across an equivalent vacuum tube is high (about 1000 volts). The resultant circuit efficiency can be as high as 96 per cent for gas tubes compared to 60 per cent or less for vacuum types. Average anode currents for gas rectifier tubes range from 0.1 to 40 amperes for the hot-cathode type, and from 5 to 400 amperes for the pool-cathode type. (The designation "hot" refers to a temperature at which radiation from the cathode is visible; such a temperature normally is attained by the application of external heat. The voltage-current operating region of the externally heated cathode type is shown in Fig. 10. A hot cathode may be heated internally by ions. However, the number of types using this principle (excluding fluorescent lamps) is negligible. A gas discharge tube in which the cathode is a pool of a liquid metal (usually mercury) is classified as a cold-cathode type of special form.) A further advantage of the gas rectifier is the superior regulation of output voltage obtainable from power supplies employing gas rectifiers. This good regulation results from the constancy of tube drop from no-load to full-load current.

The design of tubes using pool cathodes will not be considered since such types are not manufactured by RCA. However, the RCA product line does include purchased mercury-pool types.

The hot cathode of a gas tube may be either directly or indirectly heated; both types are employed in tubes presently manufactured. The directly heated cathodes have the advantages of fast warm-up time, simplicity, and low cost. The indirectly heated cathodes have the advantages of high thermal efficiency and freedom from phase effects and hum effects.

#### Cathode Efficiency

The hot cathode of a gas tube offers a much higher thermal efficiency than its vacuum counterpart because in a gas tube the anode current may be drawn from crevices and holes in the cathode surface. This phenomenon occurs because the plasma extends to within about a millimeter of the cathode surface. Thus, the emitting surface can be convoluted so that thermal radiation is conserved but electrons may emerge via the conductive plasma. Experience has shown that 1100 K is the optimum temperature for the operation of the oxide-coated cathode in a gas tube. To maintain a planar cathode at 1100 K with an emissivity of 0.25 (a value taken for barium oxide) requires 2.1 watts per square centimeter, assuming no conductivity losses. Conductivity losses and poor thermal coupling of heater and cathode may run the required power to as high as 7 watts/cm<sup>2</sup> for a cylindrical outside-coated cathode. Convoluting the cathode surface, reducing losses, heat shielding, and good thermal coupling to the heater may reduce the power required for 1100 K operation to as low as 1 watt/cm<sup>2</sup>. The indirectly heated cathode of type 3C45 (6130) (see Fig. 15) has a good thermal efficiency (3.6

watts/cm<sup>2</sup>) due to the coated insert. The indirectly heated cathode of the type 5C22 (see Fig. 16) has excellent thermal efficiency (1.56 watts/cm<sup>2</sup>) due to the fins and multiple heat shielding. Although the directly heated cathode has perfect thermal coupling between heater and cathode, other factors may prevent the attainment of high thermal efficiency. The directly heated cathode of type 5557 (see Fig. 17) (3.45 watts/cm<sup>2</sup>) does not realize optimum efficiency because most of its area can radiate to external cooler surfaces (no convolutions). The directly heated cathode of type 866A (see Fig. 18) is an improvement due to the edgewise winding of the ribbon (2.55 watts/cm<sup>2</sup>). The directly heated cathode of type 5855 (Fig. 19) (3.45 watts/cm<sup>2</sup>) has a high thermal efficiency due to the inside coating and heat shielding.

#### Cathode Design

**Average Current.** When a gas rectifier or thyatron is to be designed, the service to which it will be applied determines the average and peak cathode currents. The cathode area is a function of these currents, the type of emitting surface, and the expected life. Most gas tubes use the conventional oxide emitting surface and 2000 hours may be considered a medium life expectancy. Experience has shown that, for gas tubes using the oxide emitting surface, the average cathode-current density should not exceed 0.200 ampere per square centimeter of cathode area for a life expectancy of 2000 hours; a longer life expectancy requires a lower current density.

**Peak Current.** Consideration of peak current may require modification of the cathode area as determined by the above figure. Peak current, as used here, means the current having a duration as represented by half a sine pulse from a 60-cycle-per-second source and hav-

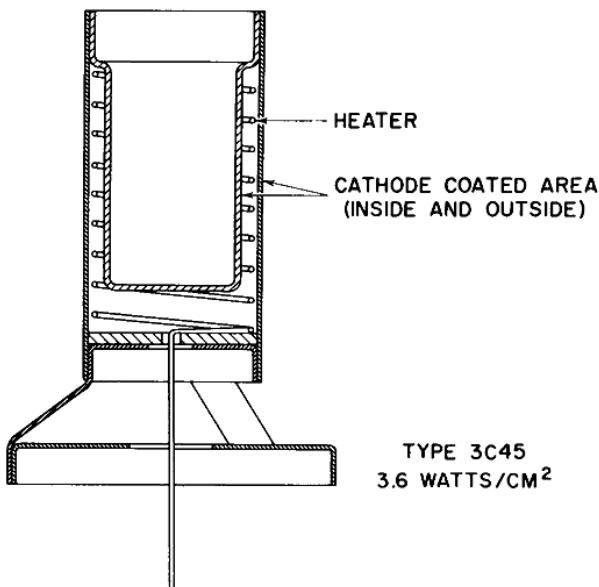


Figure 15. Indirectly Heated Cathode Structure of Type 3C45

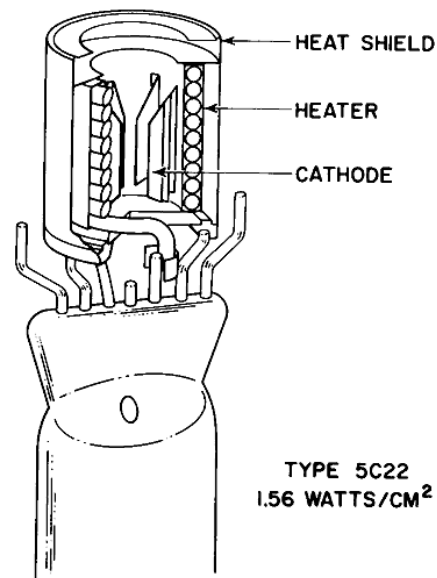


Figure 16. Indirectly Heated Cathode Structure of Type 5C22

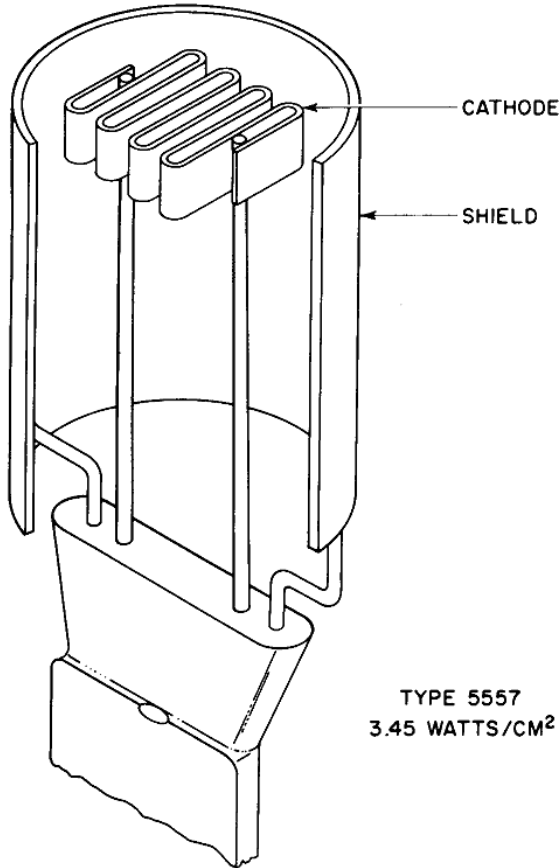


Figure 17. Directly Heated Cathode Structure of Type 5557

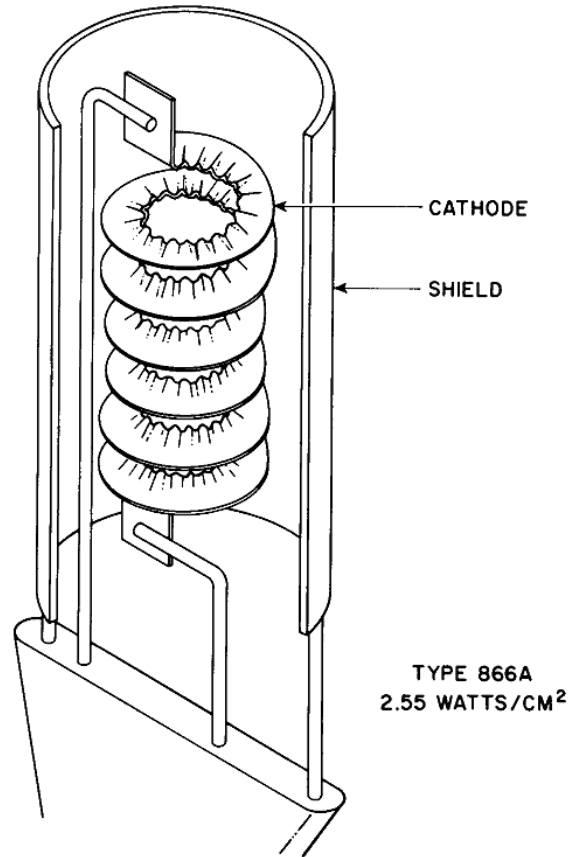


Figure 18. Directly Heated Cathode Structure of Type 866A

ing a total value of 0.008 seconds. For gas rectifiers, it has been customary to rate the peak current as four times the average current to cover the case of 180-degree conduction from a sine-wave source which yields a peak current of  $\pi$  times the average current. For industrial applications, where polyphase rectification and motor control are required, the conduction angle decreases and the ratio of peak current to average current rises. The design objective set up for thyratrons by the industry's standards organization (JEDEC) is 12.8 as the ratio of peak cathode current to average cathode current. Experience indicates that sufficient cathode area should be provided to avoid exceeding a peak current density of 2.0 amperes per square centimeter.

**Anode Voltage.** The figures for current densities given above are generally applicable to low-voltage tubes (below 2000 volts peak). Experience has shown that, for higher voltages, the current densities must be reduced to obtain the same life. The reasons for this interdependence are:

1. During the early parts of the inverse cycle of voltage, ions remain from the forward conduction cycle. These ions are accelerated toward the anode by the

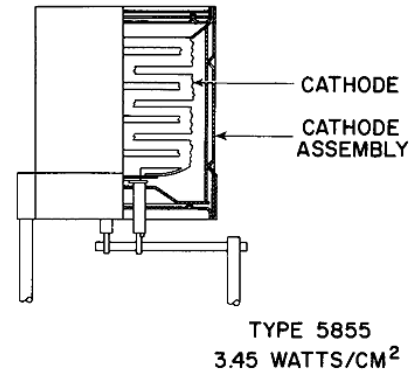


Figure 19. Directly Heated Cathode Structure of Type 5855

- high negative voltage. Upon impact, foreign gases are released which poison the cathode.
2. If sufficient ions remain during the early parts of the inverse cycle of voltage, arcbback may result.
3. The cathode current is thus limited, but not by the cathode. In the case of thyratrons, ions may be

accelerated by the high voltage during forward breakdown, and cause cathode bombardment and destruction.

**Thermal Efficiency.** After the cathode area required has been found, the power required to maintain this area at the optimum temperature of 1100 K must be determined. As described previously, the thermal efficiency of the cathode depends upon the amount of convoluting and the amount of heat shielding. The thermal efficiency is not subject to ready calculation. By comparison of a proposed structure with the samples given previously under Cathode Efficiency, one may obtain any value of thermal efficiency from 7 to 1 watt/cm<sup>2</sup>. Note, when expressed in this fashion, a low figure means a high thermal efficiency.

**Heat Shielding.** The use of a large amount of heat shielding raises the thermal efficiency but incurs the disadvantage of a long heating time. Some highly shielded cathodes require as much as 5 minutes warm-up time which is objectionably long to the customer. More moderate amounts of heat shielding are used in modern gas-tube design. The heat shields should have low thermal emissivity on both inside and outside. The power transferred by radiation from the cathode through the heat shield to the atmosphere may be expressed as

$$q = A k(T_k^4 - T_0^4) v \text{ watts}$$

where  $A$  = cathode area  
 $k$  = a constant (a function of shape)  
 $T_k$  = cathode temperature  
 $T_0$  = outside temperature

$$\text{and } v = \frac{1}{1/e_1 + 1/e_2 + 1/e_3 - 1}$$

where  $e_1$  = emissivity of cathode  
 $e_2$  = emissivity of inside heat shield  
 $e_3$  = emissivity of outside heat shield

### Heater Design

If the indirectly heated cathode is chosen for a design, power must be transferred from a high-temperature heater to a lower temperature cathode. The above formula is useful to the extent that the power is radiated, but compact designs involve power conduction, usually through an insulating layer. Power transfer by both radiation and conduction is a complex problem not unique to gas tubes. The reader is referred to other portions of this book and to a paper by Cecil E. Haller.<sup>16</sup> This discussion hereafter will be confined to the directly heated cathode.

**Voltage.** The maximum heater voltage for a gas tube is limited to that value at which an end-to-end discharge may occur across the filament. The heater voltage, because it is ac, passes through a maximum of 1.41 times the rms heater voltage at 90 degrees phase angle. At this phase angle, one end of the filament is negative and capable of emitting electrons while the other end is positive and capable of receiving electrons. A discharge ensues providing the adjacent gas path becomes ionized. This process may occur without the presence of current

to the anode. An end-to-end discharge will occur in conventional mercury tubes at heater voltages of 9 volts rms and higher; at high temperature, the resulting higher pressure lowers the threshold. This discharge may be observed on the oscillogram of heater current as a distortion of the sine wave near the peak.

By special design in which the heater is well-shielded, higher filament voltages (110 volts) may be used without showing end-to-end discharge.

**Current.** The combination of low heater voltage (2.5 volts) and high heater current is popular in modern gas tube design because large cathode currents may be permitted without appreciably affecting the heater temperature. A low instantaneous ratio of cathode currents to heater currents should be maintained at all times. In addition, the resulting low-resistance heater circuit permits the cathode current and the filament current to flow simultaneously without encountering high voltage drops. After the heater power and voltage have been determined the heater current may be calculated by using the equation  $I = P/E$ .

**Resistance.** The hot resistance of the heater may be calculated using Ohm's law  $R = E/I$ . The directly heated cathode is generally in the form of a ribbon which gives a maximum ratio of surface to volume. The following formula gives the length of the filament:

$$L = \left( \frac{RA^2}{4PB} \right)^{1/3}$$

where  $A$  = emitting area, both sides  
 $R$  = hot resistance of filament  
 $P$  = resistivity of filament material  
 $B$  = ratio of width to thickness of ribbon.

Because the ribbon is made by rolling wire, the higher the value of  $B$ , the more expensive the ribbon.  $B$  has a maximum value of 40 for most materials. The width  $W$  can be determined from the formula  $W = A/2L$ .

In the manufacture of a filament similar to that of type 866A (Fig. 18) it is necessary to crimp the ribbon before winding it by threading it through a set of gears. Such crimping distorts the ribbon cross section so that the resistance may rise 5 to 10 per cent.

Experience has shown that to produce a directly heated filament from pure nickel for the standard low filament voltages of 2.5 to 5.0 volts requires such thin material that the strength is inadequate for conventional use. The resistivity of chemically pure nickel at the normal operating temperature of 837 C is  $44 \times 10^{-6}$  ohm-centimeter. The addition of cobalt to form a nickel-cobalt alloy raises the resistivity. An alloy of 40 per cent cobalt and 60 per cent nickel (known as RCA N97 material), which has a resistivity of  $87 \times 10^{-6}$  ohm-centimeters, is commonly used for directly-heated cathodes of gas tubes. For design purposes, the cold resistance of N97 material is  $13.8 \times 10^{-6}$  ohm-centimeter.

### Gas Filling

**Choice of Gas.** Referring to Table II,<sup>17,18</sup> it may be observed that the alkali metals Cs, Rb, K, Na, Li,

offer a possible choice of gas filling since they exhibit some vapor pressure at a typical operating temperature of 100 C. The highest in this respect is mercury with cesium second. Mercury is used very successfully for the gas filling of electron tubes. Cesium has been tried on an experimental basis but no commercial tubes using it have been announced. All of the inert gases have been used for filling gas-discharge tubes or lamps. The inert gases with low ionization voltages yield the longest life in hot-cathode tubes due to the low energy of the ions that bombard the cathode. Argon was used extensively until xenon became commercially available. Because of their chemical activity or instability, other gases such as oxygen, nitrogen, carbon monoxide, and carbon dioxide are not used. Hydrogen is a notable exception. Research during World War II showed that hydrogen could be used provided exposed parts within the tube were degassed of oxygen. The amount of ion bombardment that a hot cathode can stand is described by the disintegration voltage.<sup>19</sup> The following voltages have been reported for the various gases:<sup>20</sup> mercury, -22; argon, -25; neon, -27; and hydrogen, -600.

**Clean-Up.** Another factor in determining the choice of gas for filling a gas tube is the gradual disappearance of the gas during life; this phenomenon is known as clean-up.<sup>21</sup> Gas ions, upon impact with the elements or the envelope, may remain on the surface or become imbedded within the body. The theory of gas clean-up is still incomplete, but its characteristics are well known. Gases such as nitrogen or oxygen clean up readily. For the noble gases, clean-up decreases with increasing weight. Xenon, because it is the heaviest, finds almost universal use. The low pressure (less than 100 microns) made necessary by the high inverse voltage ratings of gas tubes makes clean-up a severe problem. Clean-up may be reduced in a hot-cathode gas tube by reducing the anode-cathode spacing and by minimizing the surface area exposed to the discharge. In other words, shielding the discharge from exposure to wall surfaces of the envelope reduces clean-up. Operating conditions affect clean-up which increases with increasing inverse voltage, increasing forward current, and increasing frequency. During the time immediately following forward current conduction, ions remain within the envelope (see Fig. 20). The number of these ions is directly proportional to the electron current flowing prior to cessation of forward current (time T, Fig. 20). The energy with which these ions bombard exposed surfaces is proportional to the inverse voltage. This process, having a duration of 10 to 100 microseconds, occurs every cycle and, thus, clean-up is proportional to frequency. Average life expectancy, which is an inverse measure of clean-up, is given in Table III for typical xenon-filled rectifiers for 420 cycles per second.

**Sputtering.** Sputtering is the removal of particles of the incident surface by the bombarding ions. Generally, gas clean-up is quite severe when accompanied by sputtering. Studies of sputtering have shown there is a threshold of voltage, characteristic of each metal. These thresholds are shown in Table IV.<sup>22</sup> It is believed that the metals which sputter with difficulty will show the least gas clean-up.

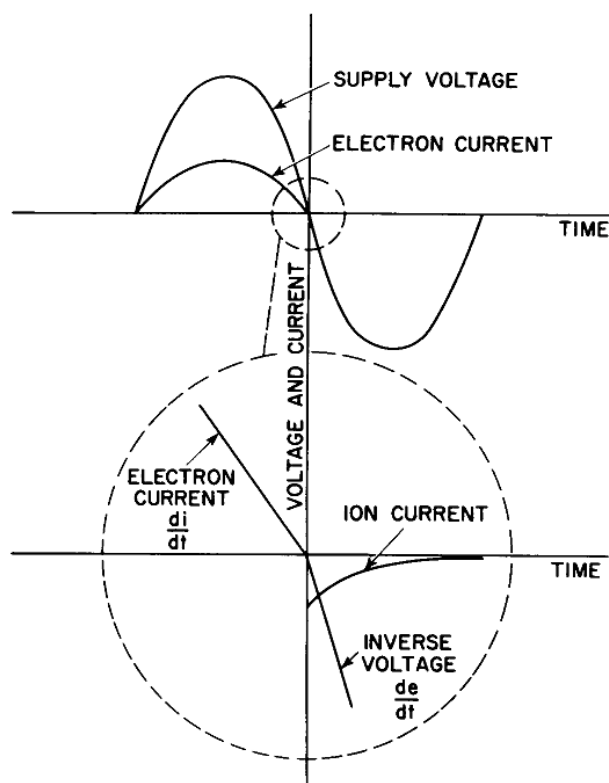


Figure 20. Commutation Factor

TABLE III. Average Life Expectancy

Type	Design	Inverse Voltage Kilovolts	Average Forward Current Amperes	Average Life Expectancy Hours
3B25	Unshielded	4.5 Kv	0.5	5000
3B28	Shielded	10.0	0.25	2000

For anode material, gas tubes employ copper, iron with zirconium spray, nickel, molybdenum, and tantalum. Copper, although subject to sputtering, is used due to its high thermal conductivity.

**Poisoning.** In addition to sputtering, another effect may occur when ions bombard a surface in a gas tube. Foreign gases which will poison the cathode may be ejected. An ion current of 1 milliamperes bombarding a previously degassed nickel surface at 250 volts acceleration will poison a 1-square-centimeter cathode surface in 2-1/2 hours. This poisoning effect has been demonstrated with the type 2050 thyratron.<sup>23</sup>

**Circuit Cushioning.** Circuit cushioning is used to minimize the harmful effects of ion bombardment. In Fig. 20, the inverse voltage reaches an appreciable

TABLE IV.  
Sputtering Threshold Voltages for Metals<sup>22</sup>

Metal	Volts
Columbium	99.8
Tantalum	97.1
Aluminum	90.8
Hafnium	90.7
Tungsten	89.5
Yttrium	89.0
Titanium	85.5
Molybdenum	76.5
Zirconium	72.8
Cobalt	70.3
Nickel	67.6
Iron	66.2
Rhodium	64.5
Chromium	55.7
Platinum	54.7
Copper	52.5
Palladium	42.0
Gold	36.2
Silver	33.4
Platinum	19.9

value before the ion current has decayed to a negligible value. The use of a combination of resistor and capacitor in series across a gas rectifier, will reduce the rate of rise of inverse voltage. Such a circuit is called a cushioning, or snubber, circuit.<sup>24</sup> The severity of ion bombardment is described partially by the commutation factor which is defined as the rate of fall of electron current  $di/dt$  (Fig. 20) multiplied by the rate of rise of inverse voltage  $de/dt$ . Many commercial tube types have been rated to withstand some maximum commutation factor. The use of these tubes must be restricted to circuits having commutation factors<sup>25</sup> within these limits.

The commutation factor depends upon tube design. The 5685 (6.4 amperes and 770 volts) with its open structure will stand only 0.66 volt-amperes per microsecond squared, whereas the close-spaced 6807 (6.4 amperes and 1500 volts) will take 130 volt-amperes per microsecond squared. To date commutation factor rating has been applied only to triodes, but it is equally applicable to diodes. To design for a high commutation factor requires that the following principles be incorporated:

- (a) Use close spacing between anode and cathode or grid.
- (b) Enclose discharge to restrict bombarding area.
- (c) Degas bombarding areas well by r-f or by ion bombardment while on the pumps.
- (d) For bombarded areas, use materials which resist sputtering.
- (e) Use gas which does not clean up readily.

**Reservoir.** A reservoir may be used to overcome gas clean-up. The mercury tube has a natural reservoir in the drop of liquid mercury with which the tube is dosed. There is clean-up in a mercury tube but it is never observed because the liquid is capable of providing many fillings of gas. For example, in type 816 only 0.01 milligram of mercury is required to fill the tube to 25 microns pressure (60 C), but the average liquid<sup>26</sup> mercury content is 500 milligrams. The absorption and desorption characteristics of hydrogen by various metals permit the design of a reservoir for the hydrogen-filled tube. Although hydrogen reservoirs have been described using various metals such as zirconium, titanium, tantalum, cesium, and lanthanum, titanium has become the most popular. One gram of titanium can be loaded with 300 liter-millimeters of hydrogen which, if it all were available, could replace the gas in a liter-volume tube 300 times to a pressure of 1 millimeter; (0.6 millimeter is typical pressure in a hydrogen-filled tube). In practice, the reservoir operates as a ballast to maintain the pressure at the desired value by absorbing or desorbing as necessary. The equilibrium value is determined by the temperature of the reservoir. (A typical temperature is 400 C.)<sup>27</sup>

**Dosing.** Several methods are available for dosing or filling the tube with the chosen gas. If the filling is done in the gaseous state at room temperature, the source may be spectroscopically pure gas commercially available in flasks of 1/4 to 1 liter at atmospheric pressure. Two stopcocks may be employed in series to dose quantities into the system. On machine exhaust, a pressure regulator reduces the pressure to about 100 millimeters; a rotating valve permits further expansion to give a dosing pressure of about 100 microns.

On trolley exhaust, a porous valve (Fig. 21) may be used for fine control of the pressure. In the position shown in the illustration, no gas leaves the supply because the mercury closes up the pores. When the upper plug is brought in contact with the lower plug, mercury is squeezed out from between the two plugs and gas passes from the high pressure source slowly into the system. The rate can be held as low as 10 liter-microns per second. For hydrogen dosing, the palladium needle method is accurate and safe. In this method (see Fig. 22), forming gas (10% H<sub>2</sub> in N<sub>2</sub>) is passed around the palladium needle which, when cold, is quite impervious to all gases. Application of power to the tungsten filament raises the temperature of the palladium needle which then becomes pervious only to hydrogen. In this manner, very pure hydrogen is admitted to the system at a controllable rate.

Several methods are in use for dosing mercury into tubes. In high-production low-cost tubes, the mercury is dosed through the exhaust tubulation by compressed air before evacuation. A surplus of mercury is dosed in this manner to cover the loss during bakeout and radio-frequency treatment. More accurate control over the final dosage is the hand-in-the-pellet method. In this method, mercury is contained in a glass or metal pellet which is attached to the mount before main sealing. In the later steps of the exhaust cycle, the mercury is released by cracking or exploding the pellet with radio-frequency current. European practice includes

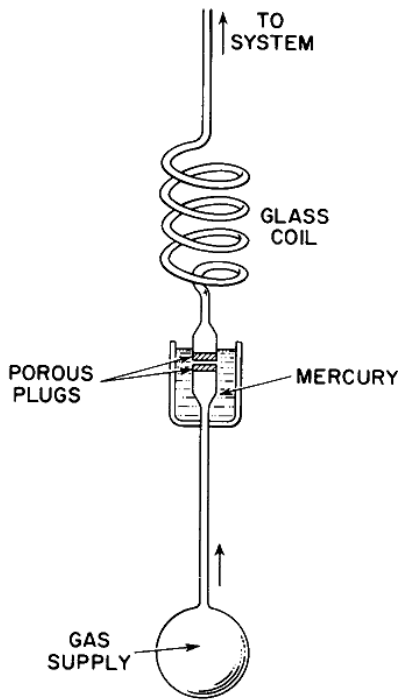


Figure 21. Porous Plug Valve

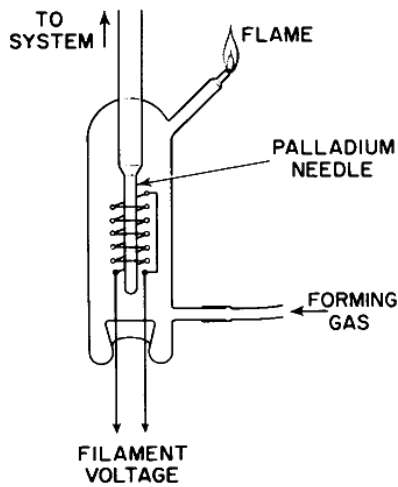


Figure 22. Palladium Needle Doser

a further refinement: a pellet containing mercuric oxide, zirconium, and iron is flashed at 500 C to decompose the oxide and release the mercury. The oxygen is gettered by the zirconium to avoid cathode poisoning.

**Pressure.** Paschen's Law (see Fig. 9) is a determining factor of the pressure to which a tube is dosed. To obtain a high operating voltage, the pressure must be above or below the minimum abscissa of Paschen's

Law. Tubes dosed above the minimum exhibit a long deionization time which limits their usefulness even at 60 cycle-per-second operating frequency. Hence, practically all hot-cathode gas tubes are dosed below the minimum of Paschen's Law. For example, to raise the arc-back voltage of a xenon-filled tube to 1000 volts, the pressure-distance product must be less than 0.5 millimeter Hg-centimeter. Maximum long path between anode and cathode may be 2 centimeters which means the maximum dosing pressure is 0.25 millimeters or 250 microns.

In the case of mercury there is no control over the dosing pressure, but the operating pressure may be controlled by controlling the temperature of the liquid. The coolest surface inside the tube will condense the vapor to a liquid and will therefore be the critical temperature. Fig. 23 shows the relationship between the vapor pressure and liquid temperature of mercury.

Anode Design

The power input to a gas tube is the product of the tube drop and the cathode current. The electrons entering the discharge at the cathode have a very low probability of reaching the anode without a collision. In Fig. 5 it is shown that an electron accelerated to 10 volts in mercury vapor will have about 60 collisions in 1 centimeter. The electrons which are collected by the anode have been slowed down by collisions or have originated in the discharge. Thus the kinetic energy of the electrons collected by the anode is less than 10 volts. The average anode heating is about 5 watts per ampere,<sup>28</sup> depending upon the anode material and area relative to other surfaces exposed to the discharge. The remaining power is removed from the discharge by

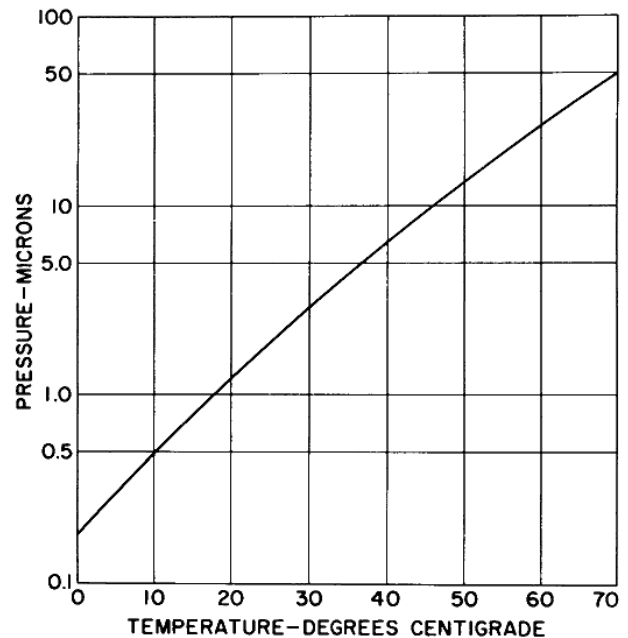


Figure 23. Vapor Pressure of Mercury

the ions and by radiation. Various materials are used for the anodes of gas tubes depending upon the application of the tube. For a rectifier where high thermal emission and low secondary emission caused by ion bombardment are important, carbonized nickel is a favorite material. Carbonized nickel which has thermal emissivity of 0.7 and operates at 300 C will radiate 0.37 watts per square centimeter. If the anode heating figure above is used the calculated anode area is 13.5 square centimeters per ampere. For carbon anodes, where the operating temperature may be considerably higher, one square centimeter per ampere is permissible. Tantalum and molybdenum are used for anode material of gas tubes because these materials resist the effects of ion bombardment on the inverse cycle (see Table IV) and have, as a result, low clean-up. Tantalum also has the advantage of gettering foreign gases when operated at about 1000 C. Zirconium is used as a coating for other metals for anodes. Zirconium hydride is mixed with iron oxide and is applied by spraying. Gettering action begins at 400 C. In one gas tube, copper has been used as an anode in order to readily conduct the heat to a radiating surface and to avoid hot spots. Other materials are described in reference 29.

#### Tube Drop

**Measurement.** If a direct current is passed through a gas tube, the voltage drop will show a constant or decreasing value as the current is increased. This effect on voltage drop results from the increase in cathode temperature caused by the increasing power injected into the discharge. Such is not the case for intermittent or periodic pulses of cathode current. Short duration pulses, i. e., one-half sine pulse from a 60 cycle-per-second source injected once per second, do not alter the cathode temperature and, therefore, give a true picture of the effect of high current on tube drop.

**Effect of Pressure.** The voltage-current characteristic of a gas discharge over many orders of magnitude of current is shown in Fig. 10. Tube drop is, by definition, the voltage across the tube, anode-to-cathode, subsequent to breakdown. Fig. 24 illustrates the manner in which tube drop varies with anode current. If the cathode is well shielded, as in the FG-166, there is a slight decrease in tube drop as current is increased from zero. After the minimum, there is a linear rise to the rated maximum peak current of the tube. In the case of an open cathode structure with little shielding (such as that of the 866A), the tube drop rises continuously from zero voltage without a minimum. The transition from the space-charge-limited current to the gas-discharge current is imperceptible. Note that at low current the tube drop is less than the ionization voltage for mercury (10.4 volts). Since the tube drop in this case is measured to the center tap, we must add half the peak filament voltage (1.75 volts) to the values given to get the peak circuit voltage. For the higher condensed mercury temperatures, the circuit voltage is still less than the ionization voltage. The explanation may be found in Fig. 11, which shows that the spacial distribution may exhibit a voltage difference greater than the circuit (cathode-to-anode) voltage.

Note, in Fig. 24, that the tube drop falls with increasing condensed mercury temperature. This fall results

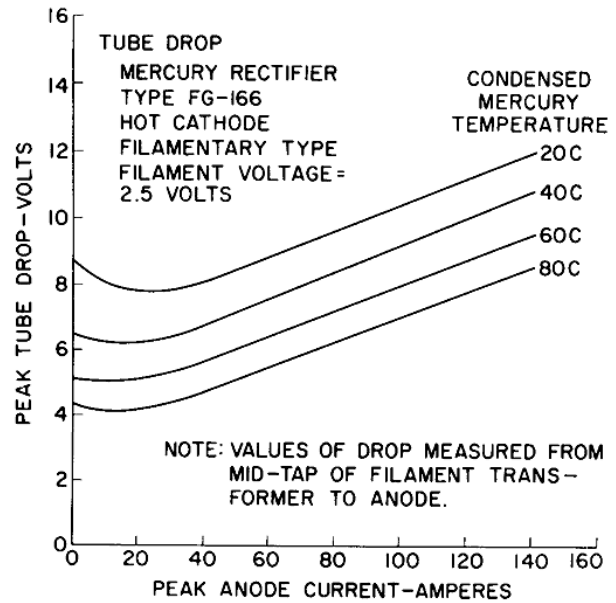


Figure 24. Tube Drop vs. Condensed Mercury Temperature

from rising mercury pressure which is accompanied by increasing probability of collision and greater ion density. A corollary to this relationship is the effect of decreasing pressure caused by clean-up in an inert gas tube. The rising tube drop increases the velocity of the positive ions. The high-speed ions may imbed themselves in the shield and cathode and thus accelerate the clean-up process. Furthermore, the rising tube drop will eventually reach the destructive sparking stage described later.

**Effect of Filament Voltage.** Fig. 25 shows how the slope of tube drop vs. current varies with the filament voltage (cathode temperature). The slope is an indicator of the quality of emission. For different cathodes operating at the same temperature, the one having the least slope has the best emission. During life the slope may fall slightly for about 100 hours, but thereafter will increase to the end of life. Fig. 26 shows how the tube drop increases as life progresses.

**Sparking.** For a given gas diode, if the pulsed cathode current is increased, the phenomenon of sparking will eventually occur. The voltage-drop trace on an oscilloscope will show a sudden discontinuity (Fig. 27) where the voltage drop will change from about 25 volts (for a xenon tube) to about 5 volts characteristic of the barium arc. Simultaneously, one or more incandescent particles can be seen in the tube flying from the cathode. Prolonged sparking will damage the cathode since a small spot of emitting area is destroyed at each spark. It has been found<sup>30</sup> that decreasing the pulse length permits higher peak currents to be drawn without sparking. Therefore, it has been concluded that the sparking results from a definite amount of energy dissipated in the cathode coating. Studies have shown that sparking

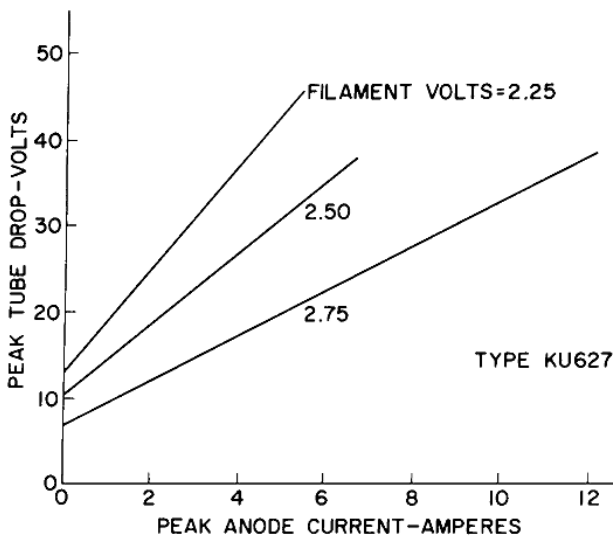


Figure 25. Tube Drop vs. Filament Voltage

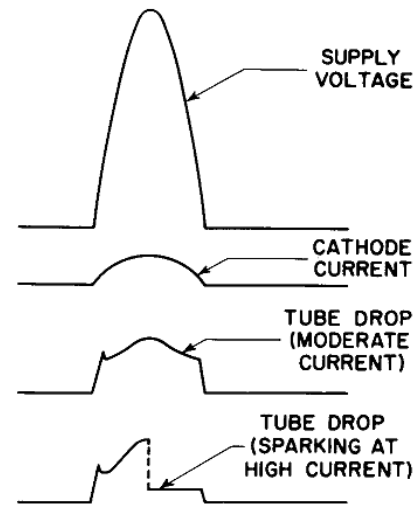


Figure 27. Sparking

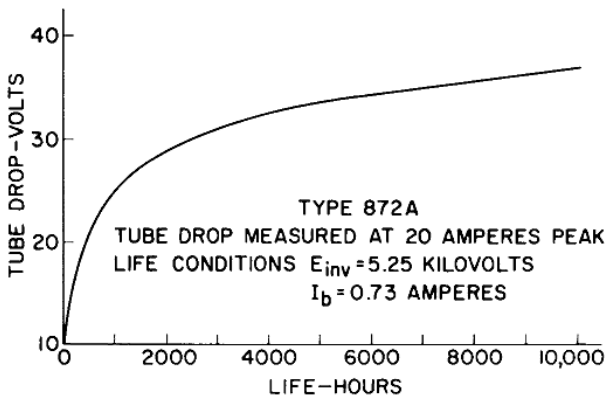


Figure 26. Tube Drop vs. Life

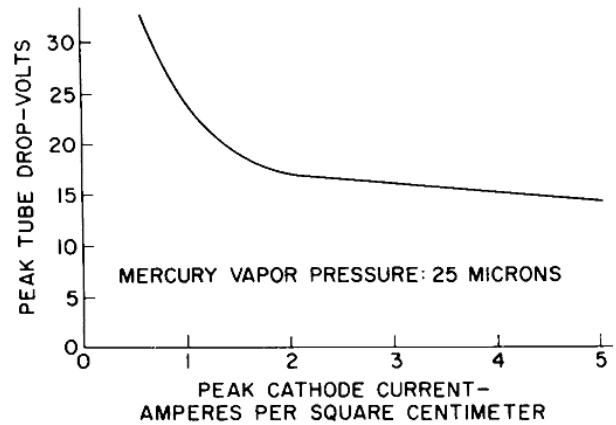


Figure 28. Sparking Limit Curve

tube drop vs. sparking current density is independent of cathode quality and filament current. Fig. 28 shows such a curve for mercury vapor at a pressure of 25 microns.

**Ion Starvation.** If the cathode in a gas diode is well shielded so that the discharge must traverse a hole of small cross section and appreciable length, another limitation on the maximum currents is encountered. The trace of voltage drop will show a discontinuity; the trace will rise to about the supply voltage and the current will cease for a short interval. Subsequently, the discharge will re-establish itself and oscillation may ensue. This phenomenon has been identified as ion starvation. The conducting path described has become starved of conducting ions. All of the gas molecules become ionized and the flow of ions to the cathode region depletes the conducting path of positive space neutralizers. The negative space charge of the electrons rises

to that characteristic of a vacuum and causes the high voltage drop. Neutral particles rush in to re-establish the arc. The sharp discontinuities play havoc with the circuitry. Ion starvation can be avoided by designing for adequate conducting paths and using sufficiently high gas pressure during operation. Fig. 29 shows results of an investigation of ion starvation on mercury tubes. <sup>31</sup>

**Fault Current.** Gas tubes are rated for average current, peak current, and fault current. The average current is largely determined by the dissipation and hence by the size of the anode and of the bulb. The peak current is primarily a function of cathode design. The fault current is the current which may be permitted perhaps a dozen times during the tube life as a result of a fault in the circuitry. Both sparking and ion starvation must be considered in the establishment of a fault-current rating. In addition, the leads must be capable of carrying the fault current.

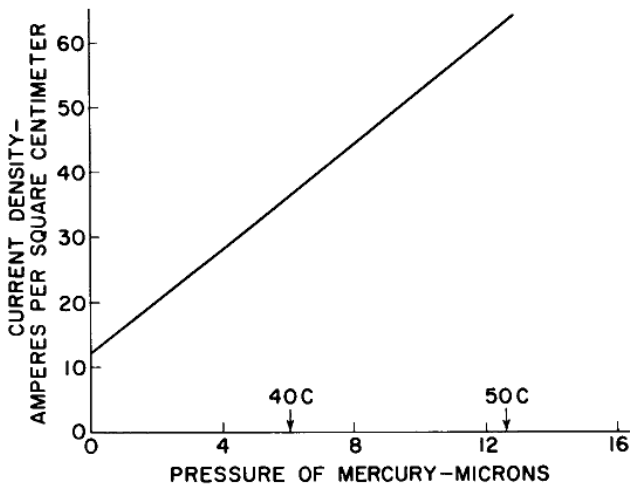


Figure 29. Ion Starvation

#### Arcback

**Pressure.** As described earlier, the breakdown of a gas between two electrodes is governed by Paschen's Law. Breakdown in the forward direction is at a low voltage because the externally heated cathode emits electrons without the aid of ion bombardment. In the reverse direction, breakdown is high because the normally cold anode will emit electrons only when bombarded by ions. Because the majority of gas rectifiers are filled to a low pressure, operation is on the lower side of the minimum of Paschen's Law.

The curve of Fig. 30 shows how the arcback voltage varies with condensed mercury temperature for the type 866A tube. Because pressure is a function of condensed mercury temperature, this curve represents the portion of Paschen's Law below the minimum. After equilibrium has been established, mercury vapor condenses on the coolest surface of the tube, and evaporation from this region determines the pressure. It is evident from Fig. 30 that high arcback voltage requires low condensed-mercury temperature. To obtain this condition, the designer must provide sufficient space and heat shields between the mercury-condensing zone and the heat-producing elements within the tube. In the type 575A, a metal disk is inserted between the cathode and the mercury-condensing zone located just above the base. In other types, such as the FG-166, the mercury condensing zone is an appendage tubing fitted with radiating fins.

The pressure in inert-gas-filled tubes is not subject to the user's control. In such tubes, the designer must select a pressure which is not so high as to cause arcback and not so low as to clean up too rapidly. A practical aspect of the arcback problem is that tubes may arc back contrary to Paschen's Law for the known mercury pressure. The reason may be the presence of a foreign gas having a Paschen's Law different from that for mercury. Limited operation at high voltage will clean up the foreign gas. Such operation is known as seasoning or high-voltage aging.

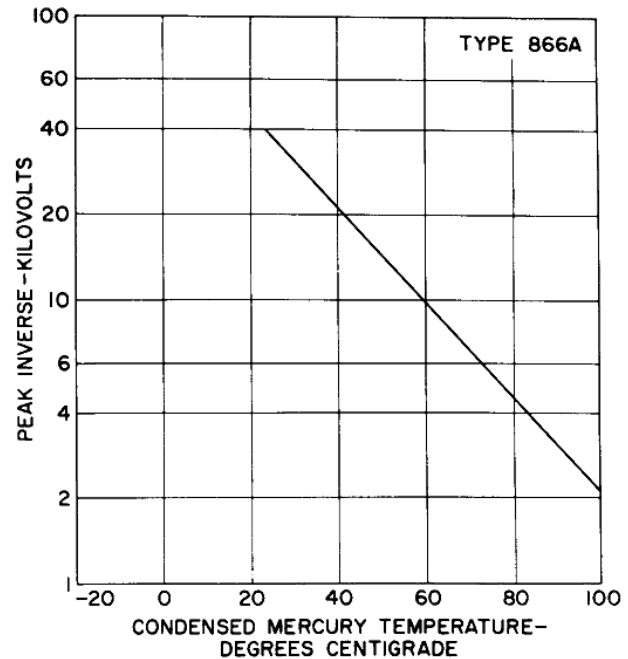


Figure 30. Arcback vs. Temperature

If not retired for preventive maintenance, all gas rectifiers fail by arcback. Verification of this statement may be found in the arcback process just described. Foreign gas, evolved from the rising tube drop accompanying emission failure, has an unfavorable Paschen's Law which results in arcback at lower than rated voltage. Reduction of dc output voltage due to the emission failure is small in high-voltage circuits. Another cause of arcback in mercury tubes is localized high pressure. A deposit of mercury on the anode (as a result of shipment or condensation) may evaporate when the tube is operated. Temporarily, the coolest surface loses control over the mercury pressure until equilibrium is re-established. Arcbacks may occur in the interim.

**Spacing.** Paschen's Law further states that, to obtain high breakdown voltage, the distance between electrodes must be small. Close spacing between the anode and cathode is not difficult to obtain, but possible long paths between the same electrodes must be eliminated. Close-fitting bulb and metal shields are employed to this end.

**Anode.** High inverse breakdown requires that electron emission from the anode be minimized. Anodes made of materials having a high work function such as carbon (4.39 volts) or iron (4.36 volts)<sup>32</sup> will have low electron emission. Practically, the material chosen must also have a high work function when contaminated with oxygen or barium. Another method of reducing arcback is to shield the cathode so as to minimize evaporation of barium onto the anode. Likewise, avoidance of severe cathode activation schedules is desirable. Aging and sparking schedules reduce arcback partly by

cleaning the anode of barium and oxygen evaporation products.

Because thermionic emission increases with temperature, a cool anode will minimize arcbacks. Shielding from the source of heat and good thermal emissivity is helpful.

The shape of the anode is important. Curved surfaces do much to reduce the electric field and thereby to raise the arcback voltage.<sup>33</sup>

**Patch Effect.** Another cause of arcback is the patch effect<sup>34</sup> in which an insulated particle on the anode surface may pick up a charge. Although the charge may be small, the minute spacing produces a large electric field — large enough to initiate field emission; the result is arcback. High-voltage seasoning or "high pott-ing" serves to burn off such particles.

**Anode Lead Design.** Good electrode design requires careful attention to the entrance and exit on the bulb for over-all success. The anode lead is particularly critical due to the enclosing high electric gradient. Paschen's Law, normally presented for linear voltage distribution, must be modified for this case. The possible arcback discharge paths originating at the anode may be interrupted by one or more glass pant legs surrounding the anode lead. Such glass pant legs (made of tubulation) must not touch the lead or each other. They also break up leakage paths. Most mercury rectifiers use one pant leg; the inert gas rectifier, 3B28, uses two pant legs, while the large inert gas rectifier, 4B32, employs three pant legs. In addition to pant legs, a reentrant structure is sometimes employed around the lead on the outside of the bulb. Fig. 31 shows a complex reentrant structure employed on the 5948 hydrogen thyatron. The path between the outer lead and the bulb, which may contain a plasma at near ground potential, is interrupted by a layer of ambient air.

THYRATRONS

Control Characteristic

**Grid.** The insertion of a third electrode, called the grid, between cathode and anode of a hot-cathode gas rectifier permits control over the forward breakdown voltage. A gas rectifier tube containing a grid is called

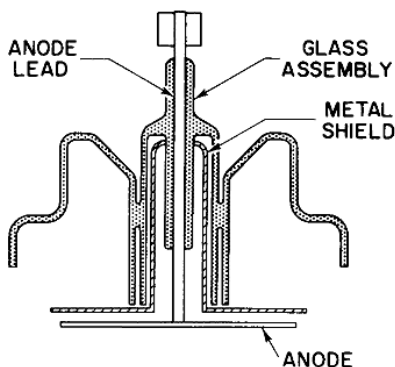


Figure 31. Reentrant Anode Lead Structure

a thyatron. Fig. 32 shows the relationship between the cathode-anode voltage  $E_a$  and the cathode-grid voltage  $E_g$  for a negative-grid thyatron. (Positive-grid thyatron design is adequately covered by United States Government research reports.)<sup>35</sup> With  $E_g$  at zero, the cathode-to-anode breakdown voltage at point a (Fig. 32) is the same as if the grid did not exist. As the grid is made more negative, the breakdown voltage ( $E_a$ ) increases linearly. The portion of the curve between points a and c is the useful region. A small voltage on the grid (tens of volts) may hold off a large voltage on the anode (thousand of volts). The curve is shaded because it does not represent a function relationship between  $E_g$  and  $E_a$  but rather a dividing line between two regions. Starting below the line, there is no breakdown and no conduction of current between cathode and anode. Raising either quantity  $E_a$  or  $E_g$  in a positive direction takes a point on the graph across the curve whereupon breakdown suddenly occurs. Recrossing the curve in the reverse direction does not restore the nonconducting condition; the reason for this lack of restoration will become apparent as grid current is studied. In other words, the grid of a thyatron is able to start conduction but is not able to interrupt conduction or to vary the amount of current. The exceptional cases and constructions whereby the grid may perform the latter functions is beyond the scope of this treatment.<sup>36, 37</sup>

The slope of the useful portion of the control characteristic (a to c, Fig. 32) is defined as the control ratio, analogous to amplification factor in a vacuum triode. The analogy is restricted to the case where the parameter, anode current, is negligibly small.

The maximum positive anode voltage rating of a thyatron restricts operation to the linear portion of the

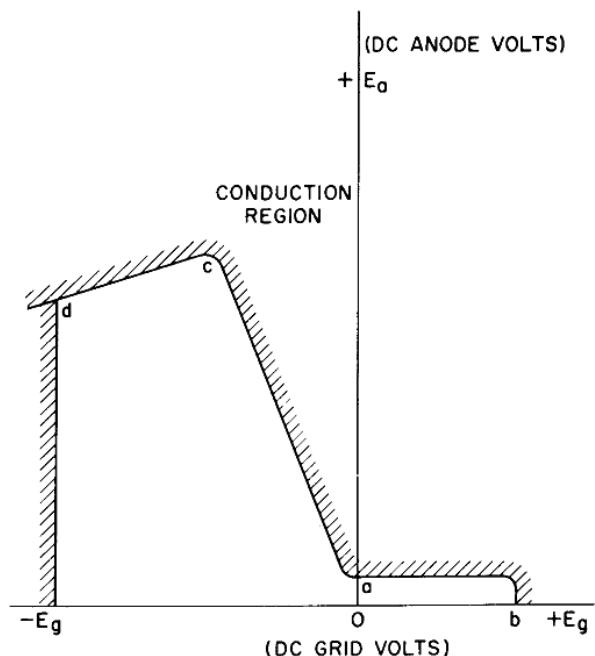


Figure 32. Thyatron Control Characteristic

control characteristic. However, if the anode voltage is increased beyond the rated maximum positive anode voltage, the grid loses control even though it be made very negative. This loss of control results from a breakdown occurring between the grid and anode in accordance with Paschen's Law; anode conduction normally follows. The downward slope (c to d) of Fig. 32 indicates that the grid-to-anode breakdown voltage is a constant value; this value is equal to the sum of the magnitudes of the two voltages referred to the cathode. The vertical line at point d is encountered when the negative grid voltage exceeds the grid-to-cathode breakdown voltage; again, this is just Paschen's Law working. In RCA Tube Division nomenclature this voltage is known as "grid glow volts." The magnitude of breakdown in the negative grid direction is several hundred volts. In the positive direction the control characteristic loses meaning when the grid-to-cathode path breaks down (point b) and the grid assumes the role of an anode. Here the magnitude is approximately equal to or less than the ionization potential (approximately 10 volts).

**Theory.** The voltage distribution in a typical thyatron before conduction is shown in Fig. 33. The space charge is negligible and, therefore, the equipotentials are the same as they would be in a vacuum tube. Fig. 34 shows the axial voltage distribution in the same thyatron before conduction. The hot cathode emits electrons of various initial velocities. All electrons with initial velocities less than that represented by the voltage minimum  $V_m$  are repelled and returned to the cathode. As the grid voltage is made less negative, a small portion of the electrons emitted are able to pass the voltage minimum and enter the grid-to-anode region. These electrons will collide with molecules producing ions and a small pre-conduction current. As the grid voltage is made less negative, the increasing number of ions begin to affect the voltage distribution (see dashed curve of Fig. 34). The positive ions have a greater effect than the electrons due to the slow speed of the ions. The rising equipotentials permit more electrons to pass and this creates more ions. Thus, the thyatron breaks down suddenly just as does a cold-cathode diode. Appendix D shows mathematically why the breakdown is sudden.

**Effect of Pressure.** In accord with Paschen's Law, the control characteristic of a thyatron is a function

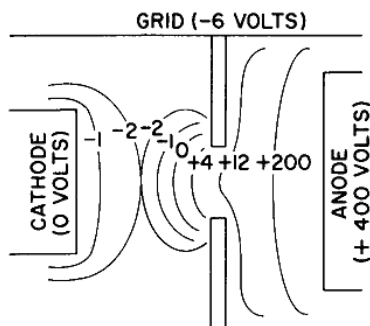


Figure 33. Equipotential Lines in Thyatron Before Conduction

of pressure. At a given grid voltage, as may be observed in Fig. 35, the thyatron breaks down at a lower anode voltage as the pressure rises. Because the dosing pressure and the maximum spacings within the tube put the operating point of thyatrons on the low side of the

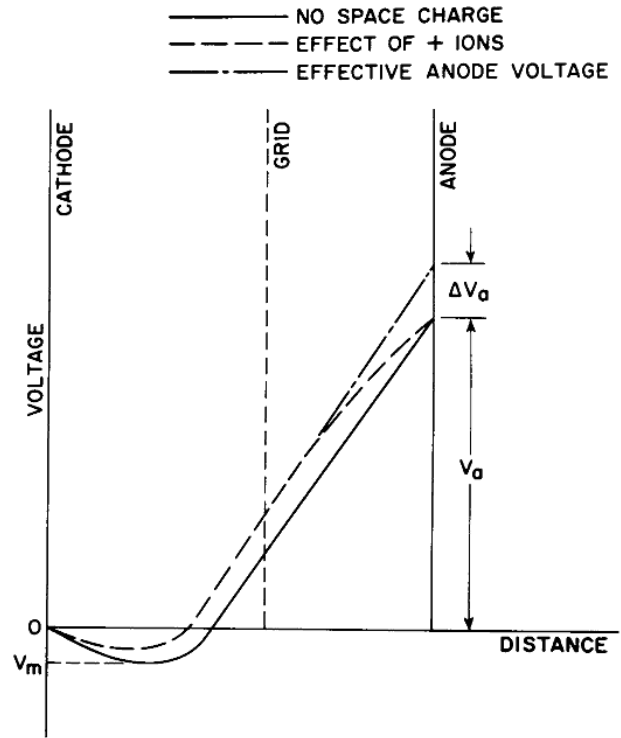


Figure 34. Axial Voltage Distribution in Thyatron Before Conduction

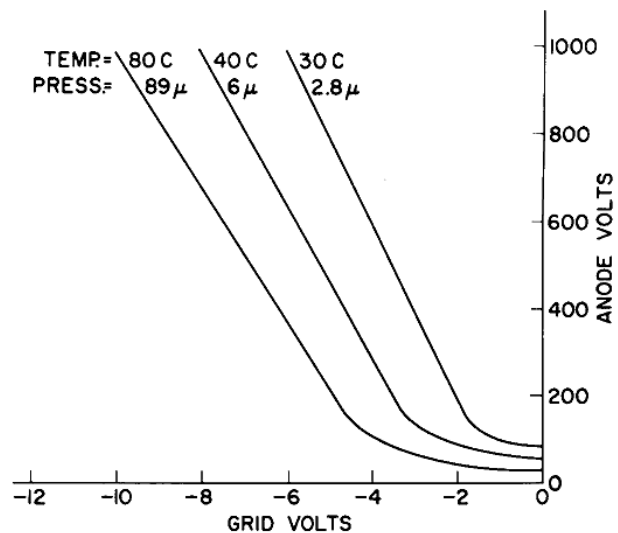


Figure 35. Control Characteristic of Thyatron at Different Pressures

minimum of Paschen's Law, it is logical to expect that thyratron breakdown would be similar to that of a gas diode.

Grid Current Prior to Conduction

**Components.** Fig. 36 shows the components which constitute grid current in a thyratron prior to conduction. Normally, the magnitude of these currents is in tenths of a microampere, but when the grid circuit resistance is in megohms, the grid currents become important. For Fig. 36, a positive dc voltage is applied to the anode. As the grid voltage is decreased from a negative value, the voltage minimum of Fig. 34 decreases in magnitude and some electrons surmount the hump. The grid collects some of these high energy electrons making up component curve 1 in Fig. 36. Many of these electrons pass through to the anode, because the grid hole (or holes) may be a large percentage of the grid cross section. The anode collects the remainder of these electrons making up curve  $I_a$ . As explained above, electrons reaching the grid-to-anode region are accelerated to ionizing velocity by the anode field and hence create ions. These ions flow in the opposite direction and are collected by the grid making up component 2 of Fig. 36; a leakage component 3 flows over the insulators on which the grid is mounted. Leakage is quite unpredictable; it generally decreases with grid voltage but may do so nonlinearly. Leakage may occur primarily to the anode, in which case it would be constant in Fig. 36. Furthermore, leakage varies with temperature. Curve 4, which represents electrons emitted by the grid, is shown as fixed since the electrons are generally attracted to the higher voltage of the anode. Likewise, grid emission is a function of temperature. Finally, capacitance current (curve 5) is shown as constant with grid voltage because most of it flows to the anode due to the higher voltage. In shield-grid thyra-

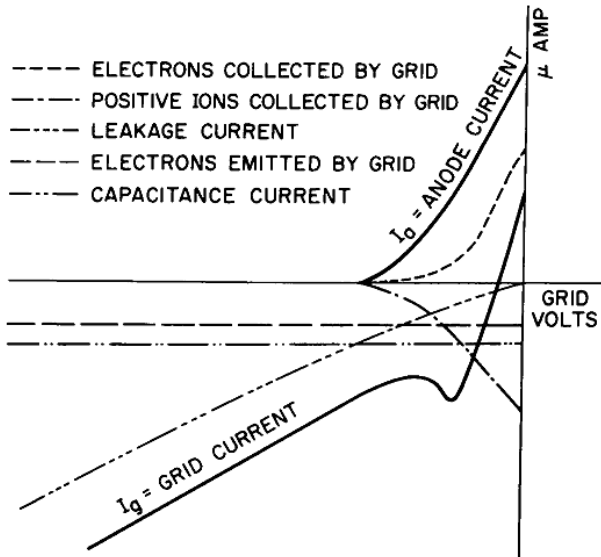


Figure 36. Components of Grid Current in Thyratron Prior to Conduction

trons, the capacitance from grid to anode, and consequently the current from grid to anode, is reduced. The resulting current  $I_g$  is the algebraic sum of all the components.

**Effect of Anode Voltage.** Fig. 37 shows the grid-current versus grid-voltage characteristic of a small thyratron (type 2050) with anode voltage as a parameter. The straight horizontal portions probably are leakage and grid emission. No capacitance current flows because the anode voltage is dc. The appearance of the ion component is quite evident as grid voltage is decreased. The small circles represent the point where breakdown occurs. Of interest is the 25-volt curve showing how the electron current to the grid predominates at low grid voltage.

**Effect of Pressure.** Fig. 38 shows the effect of pressure on the pre-conduction grid current. As the pressure is increased, the probability of collision and the amount of ionization increase. Thus, the ion current appears at a more negative grid voltage. The breakdown point is shifted to the more negative grid voltage (see also Fig. 35).

Grid Current During Conduction

**Effect of Anode Current.** The grid current of a thyratron during conduction is of the order of milliamperes

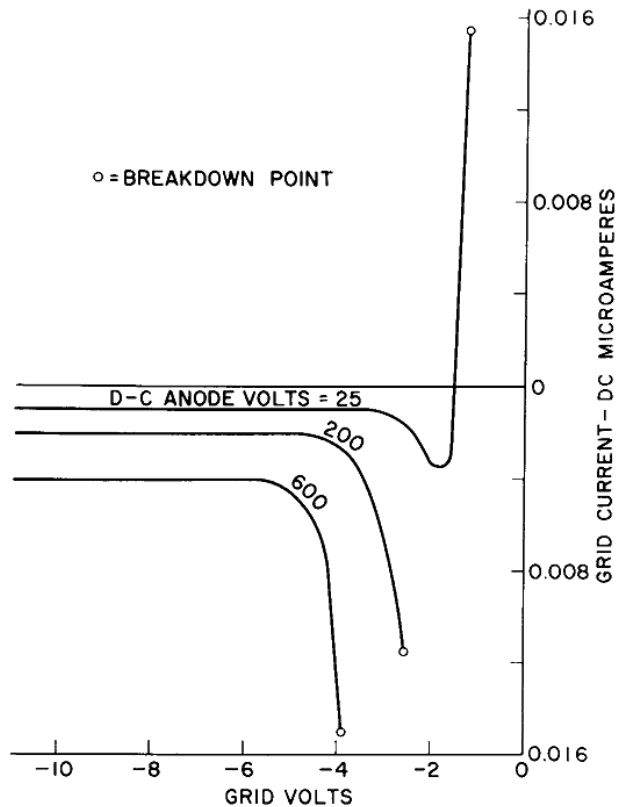


Figure 37. Grid Characteristic at Several Anode Voltages Prior to Conduction

— much greater than that measured before conduction. The grid is simply a probe in the discharge and is surrounded by a sheath across which ions flow to the grid from the plasma. The plasma has a random ion-current density determined by the anode current flowing. The flow of current is governed by the 3/2 power law. Fig. 39 shows how the grid current of a typical large thyatron (type 5563A) is saturated as the grid voltage is made more negative. As was explained earlier under "Probes," the sheath increases in thickness as the voltage increases, thus maintaining a constant current.

**Effect of Pressure.** Fig. 40 shows the grid-current versus grid-voltage characteristic with pressure as a parameter for a large thyatron (type 5563A). Although the random ion current of a plasma increases with pressure,<sup>38</sup> the voltage drop decreases (see Fig. 24) and the saturated current then decreases in accordance with the 3/2 power law.

**Design**

**Shape.** The grid of a thyatron may take many shapes. The conventional wire-wound grid of a vacuum triode functions poorly in a thyatron because the discharge may start at the edges of the coil. The grid in a thyatron must completely block all extraneous paths between cathode and anode and force the discharge through the intended aperture. The aperture may consist of holes or slots through a wall of negligible or appreciable thickness.

**Spacing.** Fig. 41 gives some data on spacing of the 5563A mercury thyatron. The grid has a single hole

of considerable depth. In general, if either the grid-to-cathode or grid-to-anode spacing is increased, the control ratio ( $\mu$ ) increases. The reason for this behavior may be deduced from the equipotential plot of Fig. 33. The field of the anode reaches through the aperture to raise the equipotentials in the grid-to-cathode space. If the anode-to-grid spacing is increased, the anode voltage is not as effective and the control ratio increases. Similarly, if the cathode-to-grid spacing is increased, the anode voltage is less effective at the cathode and the control ratio increases. This relationship is valid for the type 5563A aperture which measures 0.563 inch in diameter by 0.520 inch deep.

**Aperture Size.** Fig. 42 gives a curve of the control ratio of a small shield-grid thyatron (type 2050) for variable slot width of the grid. As the slot width is increased, the anode field becomes more effective and the control ratio, therefore, decreases.

**Material.** The prime consideration in the choice of a grid material is grid emission, which is not unique with gas tubes. Several materials are being successfully used for gas tube grids. A large thyatron (type 7086) uses a copper grid for high thermal conductivity to reduce the grid temperature. The side exposed to the cathode is sprayed with aqua-dag to reduce grid emission. A high-voltage thyatron (type 5563A) uses carbonized nickel successfully. Gold-plated grids are

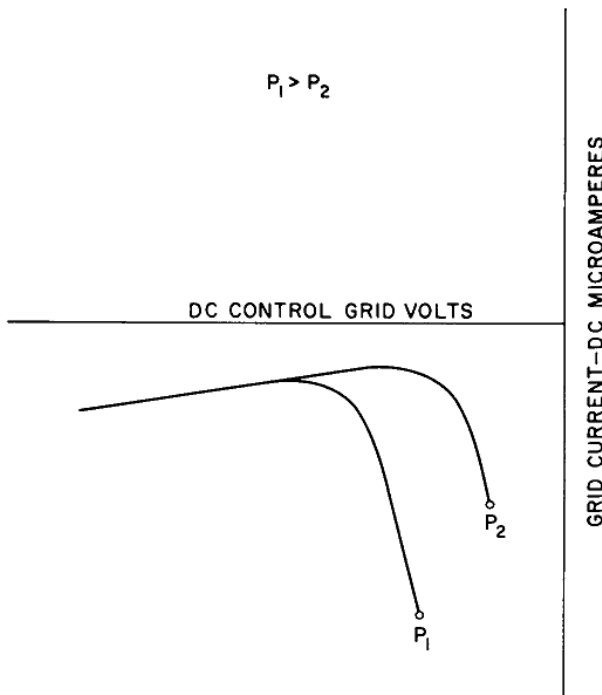


Figure 38. Grid Characteristic and Pressure Effect Prior to Conduction

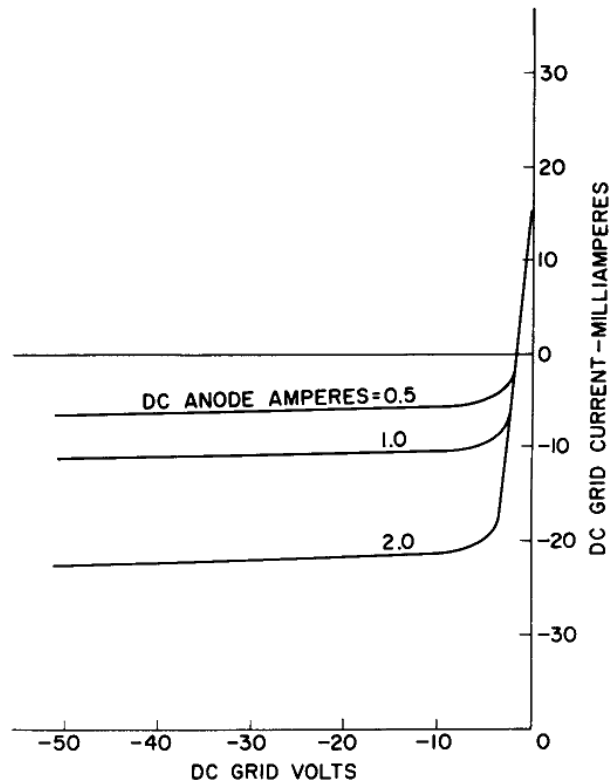


Figure 39. Grid Characteristic at Several Anode Currents During Conduction

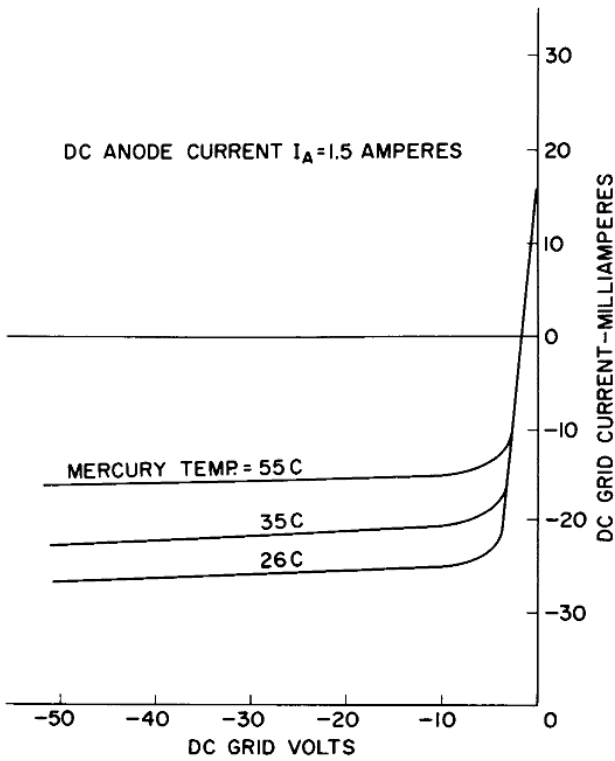


Figure 40. Grid Characteristic at Several Pressures During Conduction

used in small thyratrons, e.g., type 2050. Thyratrons merchandized by RCA, e.g., type C6J, use tungsten rods which have been heavily oxidized.

REFERENCES

1. Loeb, L. B., Kinetic Theory of Gases, 2nd Ed., p. 95., McGraw-Hill, 1934
2. Kennard, E. H., Kinetic Theory of Gases, McGraw-Hill, p. 149, 1938
3. Maxfield, F. A., and R. R. Benedict, Theory of Gaseous Conduction and Electronics, McGraw-Hill, p. 116, 1941
4. Parker, P., Electronics, E. Arnold Co., p. 581, 1950
5. Parker, P., op. cit.
6. Ibid., p. 591
7. Ibid., p. 593
8. Maxfield and Benedict, op. cit., p. 169
9. Druyvesteyn, M. J., and F. M. Penning, "The Mechanism of Electrical Discharges in Gases at Low Pressure," Rev. Mod. Phys., 12, 148, April 1940
10. Malter, L., E. O. Johnson, W. M. Webster, "Studies of Externally Heated Hot Cathode Arcs," RCA Review, 12, 417, September 1951
11. Applied Electronics, M. I. T. Staff, John Wiley, p. 120, 238, 1943
12. Wheatcroft, E. L. E., Gaseous Electrical Conductors Oxford Univ. Press, London, p. 187, 1938

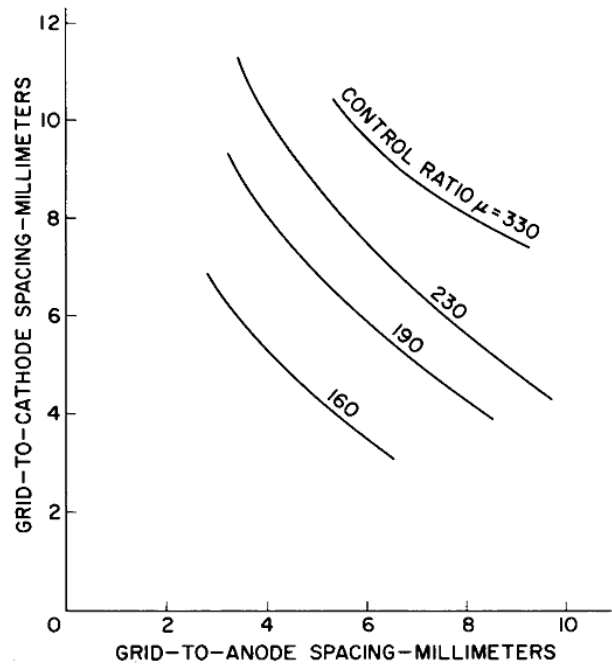


Figure 41. Control Ratio vs. Spacing

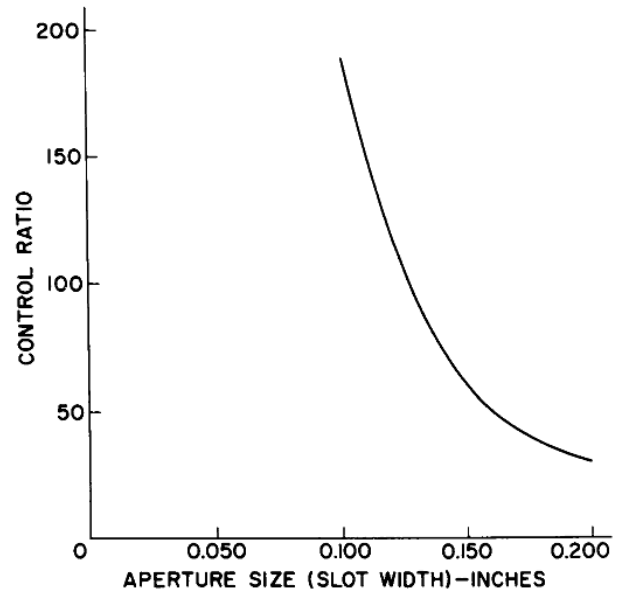


Figure 42. Control Ratio vs. Aperture (Slot) Size

13. Parker, P., op. cit., p. 1004
14. Parker, P., op. cit., p. 944
15. Maxfield and Benedict, op. cit., p. 118
16. Haller, E., "Filament and Heater Characteristics," Electronics, July 1944
17. Wheatcroft, op. cit., p. 30
18. Handbook of Chemistry and Physics, Chemical

- Rubber Publishing Co., Cleveland, Ohio, 35th Edition
19. Hull, A. W., "Gas Filled Thermionic Tubes" A.I.E.E. Trans., 47, 753, 1928
  20. Pulse Generators, M. I. T. Staff, McGraw-Hill, p. 336, 1948
  21. Reddan, M. J., and G. F. Rouse, "Clean-up of Helium Gas in Arc Discharge," E.E. v. 71, 159, 1952
  22. Code Q1
  23. Code Q2
  24. Edwards, D. V. and E. K. Smith, "Circuit Cushioning of Gas-Filled Grid-Control Rectifiers," A.I.E.E. Trans., 65, 640, Oct. 1946
  25. Code Q3
  26. Code Q4
  27. Murphy, J. A., "Zirconium and Titanium Gas Reservoirs for Hydrogen Thyratrons," General Electric Co., Electronics Dept. Report 52E715, (8-12-52)
  28. Wheatcroft, op. cit., p. 214
  29. Spitzer, E. E., "Anode Materials for High Vacuum Tubes," E. E., Nov. 1935
  30. Knowles, D. D., and J. W. McNall, "Sparking of Oxide Coated Cathodes in Mercury Vapor," J.A.P., 12, 149, Feb. 1941
  31. Hull, A. W., and F. R. Elder, "The Cause of High Voltage Surges in Rectifier Circuits," J. A. P., 13, 372, June 1942
  32. Reference Data for Radio Engineers, I. T. & T. Corp., 4th Ed., p. 43, 1956
  33. RCA Bulletin, Types 6894, 6895
  34. Cranberry, Louis, "Patch Theory of Arcback," J. A. P., 23, 518, May 1952
  35. Goldberg, Seymour, Research Study on Hydrogen Thyratrons, Edgerton, Germeshausen, and Grier, Inc., Boston, Mass., Vol. I and II, 1956
  36. Johnson, E. O., "Controllable Gas Diode," Electronics, 24, 107, May 1951
  37. Knight, H. de B., "Hot Cathode Thyratrons," P.I.E.E. 96, 371, Sept. 1949
  38. Parker, P., op. cit., p. 644
  39. Hermann, G. and Wagener, S., Oxide-Coated Cathodes, Chapman & Hall, Vol. I, p. 78

APPENDIX A. BREAKDOWN

- Let  $I_0$  = number of electrons leaving negative electrode per second
- $\alpha$  = ions or electrons produced per centimeter travel of electron
- $I_a$  = electron current reaching the positive electrode (anode)
- $x_a$  = distance negative to positive electrodes
- $I_p$  = primary electrons leaving cathode (exciting current)
- $I_+$  = positive ion current reaching cathode
- $\gamma$  = secondary electrons released at cathode per incident ion

The electron current will build up as it crosses from the negative to the positive electrode. The increment per element of path  $dx$  is:

$$dI = \alpha I dx \tag{1}$$

Separating variables and integrating gives:

$$I_a = I_0 e^{\alpha x_a} \tag{2}$$

The positive ion current reaching the negative electrode is, by subtraction:

$$I_+ = I_0 (e^{\alpha x_a} - 1) \tag{3}$$

The current  $I_0$  leaving the cathode consists of:

$$I_0 = I_p + \gamma I_+ \tag{4}$$

Combining Eqs. 2, 3, and 4:

$$I_a = \frac{I_p e^{\gamma x_a}}{1 - \gamma (e^{2x_a} - 1)} \tag{5}$$

The constants  $\gamma$ ,  $\alpha$ , and  $x_a$  may be given finite values such that the denominator becomes infinite; hence, mathematically, there can be a breakdown.

APPENDIX B. PASCHEN'S LAW

Eq. (5) of Appendix A becomes the breakdown equation when the current  $I_a$  is increased to a critical value  $cI_a$ . The variables remaining in Eq. (5) of Appendix A at breakdown are:

- $\alpha x_a$  = the product of ionizing coefficient and distance between electrodes
- $\gamma$  = the secondary emission coefficient of the cathode

The ionizing coefficient  $\alpha$  (see Fig. 5) is a function of the average number of collisions per centimeter ( $1/\lambda_e$ ) (see Fig. 4) and the kinetic energy  $V$  of the colliding electron.

$$\text{thus } \alpha = f_1 \left( \frac{1}{\lambda_e} \right) f_2 (V) \tag{1}$$

where  $\lambda_e$  is the mean free path of the electron

Substituting for  $V$

$$\alpha = f_1 \left( \frac{1}{\lambda_e} \right) f_2 \left( \frac{V_a \lambda_e}{x_a} \right) \tag{2}$$

where  $V_a$  is the voltage between electrodes

Although  $\lambda_e$  varies with voltage, as Fig. 4 shows, above about 10 volts  $\lambda_e$  approaches the kinetic theory value and can be considered a constant. As the pressure is changed,  $\lambda_e$  varies inversely.

Substituting

$$\alpha = f_1(p) f_2 \left( \frac{V_a}{X_a P} \right) \tag{3}$$

Multiplying by  $X_a$

$$\alpha X_a = f_3 (X_a P) f_2 \left( \frac{V_a}{X_a P} \right) \tag{4}$$

Thus one variable  $\alpha X_a$  in the instability (Eq. (5) of Appendix A) above has been reduced to functions of  $X_a P$  and  $V_a$ .

The secondary emission coefficient  $\gamma$  is a function only of the energy with which the ion strikes the cathode

$$\gamma = f_4 \left( \frac{\lambda_i V_a}{X_a} \right) \tag{5}$$

where  $\lambda_i$  is the mean free path of ion.

Like  $\lambda_e$ ,  $\lambda_i$  varies inversely with pressure

$$\gamma = f_5 \left( \frac{V_a}{X_a P} \right) \tag{6}$$

Thus the variables of the breakdown equation have been reduced to  $V_a$  and  $X_a P$ ; the equation relating these two variables is Paschen's Law.

APPENDIX C. COLLISION OF ELECTRON AND ION

$$\frac{M_1 v_1^2}{2} = \frac{M_1 V_1^2}{2} + \frac{M_2 V_2^2}{2} \tag{1}$$

$$M_1 v_1 = M_1 V_1 + M_2 V_2 \tag{2}$$

- where  $M_1$  = mass of electron
- $M_2$  = mass of ion
- $v_1$  = velocity of electron before impact
- $V_1$  = velocity of electron after impact
- $V_2$  = velocity of ion after impact

Solving these two equations for the kinetic energy after impact of the electron gives:

$$W_1 = \left( 1 - \frac{2M_2}{M_1 + M_2} \right)^2 w_1$$

$w_1$  = kinetic energy of electron before impact

$W_1$  = kinetic energy of electron after impact

Because the mass of the electron  $M_1$  is so small com-

pared to the mass of the ion  $M_2$ , the quantity in parenthesis is nearly unity and hence there is very little loss of kinetic energy by the electron in impact. For the electron to recombine, it must release all of its kinetic energy to the ion. The above relationship precludes this release and recombination is rare in the gas.

APPENDIX D. BREAKDOWN OF A THYRATRON

The solid line in Fig. 34 shows the axial voltage distribution of a thyatron without space charge. Of the electrons emitted by the cathode, only those having more kinetic energy than the potential energy of the voltage minimum pass through to the grid-anode region. Dividing both sides of Eq. (17) (An expression for the number of charged particles crossing unit area against a retarding voltage) by time converts the number to current:

$$I = I_S e^{-\frac{qV_m}{KT}} \quad (1)$$

where  $I_S$  is the total cathode emission  
 $q$  is the charge and is negative.

The potential minimum  $V_m$  is a function  $\phi$ , of  $V_g$  and  $V_a$

$$V_m = \phi \left( V_g + \frac{V_a}{\mu} \right) \quad (2)$$

$\mu =$  control ratio.

As Fig. 34 shows, positive ion space charge raises the voltage distribution by an effective amount  $\Delta V_a$ . Assume that the amount of rise  $\Delta V_a$  is proportional to the anode current  $I_a$ .

$$\text{then} \quad \Delta V_a = RI_a \quad (3)$$

where  $R$  is constant

Substituting in Eq. (1) gives:

$$I = I_S e^{-\frac{q}{KT} \phi \left( V_g + \frac{V_a + RI_a}{\mu} \right)} \quad (4)$$

Taking the logarithm of both sides

$$\ln I = \ln I_S + \frac{q}{KT} \phi \left( V_g + \frac{V_a + RI_a}{\mu} \right) \quad (5)$$

Since  $I_S$  is a constant

$$\ln I = \phi \left( V_g + \frac{V_a + RI_a}{\mu} \right) \quad (6)$$

where  $\phi$  is an unknown function

Now  $I$  is the electron current passing the voltage minimum. The anode current  $I_a$  is augmented by the ionization, but is a function of  $I$ .

Hence:

$$\ln I_a = f \left( V_g + \frac{V_a + RI_a}{\mu} \right) \quad (7)$$

Let the function  $f$  be a linear one

$$\ln I_a = K \left( V_g + \frac{V_a + RI_a}{\mu} \right) \quad (8)$$

$K =$  constant

Rearranging

$$\ln I_a - K \frac{RI_a}{\mu} = K \left( V_g + \frac{V_a}{\mu} \right) \quad (9)$$

Taking the derivative of Eq. (9)

$$\frac{dI_a}{dV_g} = \frac{K}{\frac{1}{I_a} \frac{KR}{\mu}} \quad (10)$$

In conclusion,  $\frac{dI_a}{dV_g}$  becomes infinite when  $1/I_a = -KR/\mu$ ;  $I_a$  is no longer limited by  $V_g$  and breakdown occurs.